INTER-TANGLED NETWORK OF POLYMERS FOR ULTRAFAST RECHARGEABLE BATTERIES

Jieun Kim

Department of Energy Engineering
Graduate School of UNIST

2014

INTER-TANGLED NETWORK OF POLYMERS FOR ULTRAFAST RECHARGEABLE BATTERIES

A thesis
submitted to the Graduate School of UNIST
in partial fulfillment of the
requirements for the degree of
Doctor of Philosophy/Master of Science

Jieun Kim

01. 27. 2014

Approved by

Major Advisor
Hyun-Kon Song

INTER-TANGLED NETWORK OF POLYMERS FOR ULTRAFAST RECHARGEABLE BATTERIES

Jieun Kim

This certifies that the thesis of Jieun Kim is approved.

01. 27. 2014

Signature

Thesis supervisor: Hyun-Kon Song

Signature

Changduk Yang

Tae-Hyuk Kwon

Abstract

Metal oxides such as $LiCoO_2$ and $LiMn_2O_4$ have been widely used as cathode materials of lithium ion batteries. The inorganic compounds provide practically high capacity based on the redox activity of d orbital transition metals with structural stability leading to cycle retention. As a logical alternative to the conventional cathode materials, also, organic cathode materials have attracted academic attentions from the viewpoint of (1) unlimited elemental resources and (2) elastic properties guaranteeing flexibility in case of polymeric materials. In this work, poly (vinyl carbazole) (PVK) was studied as an electro-active material for cathode materials of lithium ion batteries. PVK showed binder and conductive agent-dependent performances probably because of its volumetric change during oxidation. More elastic polymer binder and use of carbon nanotubes as a conductive agent guaranteed higher capacity (~120 mAh g^{-1} at 0.1C) and enhanced rate capability (up to several hundreds of C-rate). Optimized condition for making electrode composites would allow practical application of PVK to cathode materials for rechargeable batteries.

Moreover, A 1D organic redox-active material is composited with another 1D conductive material for rechargeable batteries. Poly (vinyl carbazole) (or PVK) and Poly(3,4-ethylenedioxythiophene) doped with poly(styrenesulfonate) (or PEDOT:PSS) are used as the redox-active and conductive 1D materials, respectively. Due to their extreme anisotropic geometry, the two polymers are expected to be inter-tangled with each other, showing an kinetically ideal model system in which each redox-active moiety of PVK is supposed to be directly connected with the conducting pathways of PEDOT:PSS. In addition to the role of conductive agents providing kinetic benefits, PEDOT:PSS works as an efficient binder that guarantees enhanced electrochemical performances with only a tenth of the amount of a conventional binder (polyvinylidene fluoride or PVdF). The benefit of gravimetric energy density gain obtained with the conductive binder comes mainly from efficient spatial coverage of binding volume due to the low density of PEDOT:PSS. Towards realizing flexible all-polymer batteries, a quasi-all-polymer battery half-cell is designed with the PVK/ PEDOT:PSS composite with a polymer gel electrolyte.

Contents

List of figures

containing 0.1 M $TBAClO_4$. (c) The PTMA/SWNT (black circle) and PTMA (white circle) composite electrodes capacity during discharge processes.

Figure. 11. Structure and discharge profile of DCA as an active material with two step reaction.

Figure. 12. CV of chloranil as an active material in the system of dilute sulphuric acid. Scan rate= 0.33 mV s^{-1}.

Figure. 13. Discharge curves of chloranil in dilute sulphuric acid with diverse C-rate. (Potential vs. SCE)

Figure. 14. Discharge curves of chloranil in ammonium chloride solution with diverse C-rate. (Potential vs. SCE)

Figure. 15. CV of chloranil as an active material in the system of ammonium chloride electrolyte. Scan rate= 0.33 mV s^{-1}.

Figure. 16. Top; The creation of polymeric 1, 4-dimethozxybenzene (DMB) from DMB. Bottom; The oxidation and reduction reaction of PDMB film on stainless steel electrode. Then, filtered and washed with acetonitrile to remove PDMB from the electrode. Li metal as a counter and reference electrode. 0.5 M $LiClO_4$ in PC containing excess DMB was used as an electrolyte. Scan rate= 50 mV s^{-1}.

Figure. 17. The first cycle profiles of PQ with carbon in $LiAsF_6$ in THF electrolyte.

Figure. 18. The first and second discharge curves at 0.1 mA cm^2.

Figure. 19. CV with basic material, anthraquinone, of NBHQ. Scan rate= 1 mV s^{-1}. Electrolyte= $LiClO_4$ in PC/DME (1/3 wt. %).

Figure. 20. Discharge capacity of NBHQ electrochemical cell at 0.5C during over 500 cycles. Inset figure showed a representative discharge profile.

Figure. 21. Thermal stability of PVK tested by Differential scanning calorimetry (DSC) under a hydrogen atmosphere. Heating rate= 10 ^oC min^{-1}.

Figure. 22. The cyclic voltammograms of CNT effect with variable scan rates (10, 5, 1, 0.1 mV/s).

Figure. 23. (a) Electrochemical impedance spectroscopies at peak potentials 4.2 V (vs. Li/Li^+) from 200 kHz to 0.1 Hz. All cells were measured coin-type cells. **(b)** Values are calculated by fitting program, Z view.

Figure. 24 Charge/discharge profiles of PVK as an active material and PVdF as a binder with or without CNTs. Charge= 1C-rate/ discharge= variable C-rate (1 and 10C).

Figure. 25. (a, b) The cyclic voltammograms of PVdF and PAA-CMC binder electrodes with se. Scan rate= 10 mV/s. **(c, d)** How to calculate capacity with cyclic voltammograms with scan rate (10 mV/s).

Figure. 26. (a, b) Charge/discharge profiles of composite electrodes with **(a)** PVdF and **(b)** PAA-CMC binder (charge= 1C/discharge=variable). **(c, d)** Scanning electron microscopies of electrode with PVdF of PAA-CMC binder. (The cells were not add CNTs as a secondary conducting agent)

Figure. 27. Impedance spectra with binders at peak potentials 4.2 V (vs. Li/Li^+) from 200 kHz to 0.1 Hz.

Figure. 28. Effects of CNTs as a secondary conducting agent and PVdF as a binder. (a) EIS, (b) calculated values of resistance and capacitance.

Figure. 29. Schematic picture of a tangle of PVK (red) and PEDOT:PSS (blue). Electrons are transferred from electroactive sites (red balls) of PVK to PEDOT:PSS and then moves along PEDOT:PSS strand in a fast way.

Figure. 30. Benefits of a conductive binder (PEDOT:PSS) compared with a conventional binder (PVdF). Charge transfer resistances (R) are reduced with PEDOT:PSS.

Figure. 31. Coating quality of composites based on PVdF and PEDOT binders. Aluminium foils were used as substrates. Poor adhesion was observed with 1 wt. % PVdF (b) while the composite was successfully coated with the same amount of PEDOT:PSS (c).

Figure. 32. Morphological SEM images of composite electrodes. Composites based on various PEDOT contents were compared with PVdF-containing one.

Figure. 33. Charge/discharge profiles of binder dependent performances with PVK and Super P. Charge= 1C-rate/discharge= variable.

Figure. 34. (a) Cyclic voltammograms (CVs) scanned at 10 mV s^{-1}. (b) Scan rate dependency of peak-to-peak potential gap ($\triangle E_p$).

Figure. 35. Electrochemical impedance spectra at peak potentials (4 V for PEDOT and 4.2 V for PVdF) from 200 kHz to 0.1 Hz.

Figure. 36. Capacity depending on discharge rates at a fixed charge rate (1C). Capacity was normalized by mass of PVK (a) or composites including all components such as PVK, binder and carbon black (b).

Figure. 37. Electric conductivities (σ) of PEDOT:PSS of various contents versus 10 wt. % of PVdF.

Figure. 38. PEDOT contents dependency of electrochemical performances. (a) CVs. (b) Electrochemical impedance spectra. (c) Capacity depending on discharge rates at a fixed charge rate (1C). (d) Capacity retention with cycles at 10C/10C (charge/discharge).

Figure. 39. Conductive potential window of PEDOT:PSS. (a) CV is obtained at 10 mV s^{-1}. Three pairs of peaks related to faradaic reactions are observed. (b) Electrochemical impedance spectra at various potential.

Figure. 40. Electrochemical performances of quasi-all-polymer cells of PVK, PEDOT:PSS, PVA-CN and polyolefin. Capacities depending on discharge rates at a fixed charge rate (1C) were normalized by mass of PVK (a) or composites including all components such as PVK, binder and carbon black (b).

Figure. A. 1. Mimetic diagram of coin-cell.

Figure. A. 2. FT-IR of synthesized PAQS powder. Range of wave number= 2000~650 cm^{-1}.

Figure. A. 3. The profiles of PAQS at 0.1C during the charging.

List of tables

List of Schemes

Nomenclature

AAO	Anodic aluminum oxide
AQ-*ter*-denpol	Denpol containing anthraquinone terminated dondrons
CMC	Carboxymethyl cellulose
CNTs	Carbon nanotubes
C	C-rate
CV	Cyclic voltammograms
DCA	Dichloroisocyanuric acid
DEC	Diethyl carbonate
DMC	Dimethyl carbonate
DME	Dimethoxyethane
DOL	1,3-dioxolane
EC	Ethylene carbonate
EIS	Electrochemical impedance spectroscopy
LCO	Lithium cobalt oxide
LIBs	Lithium-ion batteries
$LiPF_6$	Lithium hexafluorophosphate
NMP	N-Methyl-2-pyrrolidone
PAA	Polyacrylic acid
PANI	Poly (aniline)
PAQS	Poly (anthraquinonyl sulfide)
PC	Propylene carbonate
PEDOT:PSS	Poly(3,4-ethylenedioxythiophene): poly(styrenesulfonate)
PTMA	poly (2,2,6,6-tetramethylpiperidinyloxy methacrylate)
PVdF	Polyvinylidene fluoride
PVK	Polyvinyl carbazole
SCE	Saturated calomel electrode
SHE	Standard hydrogen electrode
SWNTs	Single-walled carbon nanotubes
TEMPO	2,2,6,6-Tetramethylpiperidin-1-oxyl
THF	Tetrahydrofuran

I. INTRODUCTION

1.1. Introduction to Rechargeable batteries

Rechargeable batteries have occupied the market of electric devices, especially portable devices, on account of their high energy and power densities. It reduce concerns of the petroleum inflation or CO_2 emission.[1-2] Some practical demands are required to develop performances including light weight, charge-discharge efficiency and cost. Lithium-ion batteries (LIBs) contain cathode, anode, electrolyte and separator. The conventional LIBs comprehend a cathode formed by a lithium metal oxide ($LiCoO_2$), a graphite anode, electrolyte consisting of a solution of a lithium salt ($LiPF_6$) in a mixed organic solvent (ethylene carbonate, dimethyl carbonate) and polyolefin separator.[3-4]

Li-ions moving between cathode and anode through the electrolyte during the electrochemical oxidation and reduction on the electrodes. At the same time, electrons flow along the external conductor and closed circuit is designed. **(Figure. 1)**

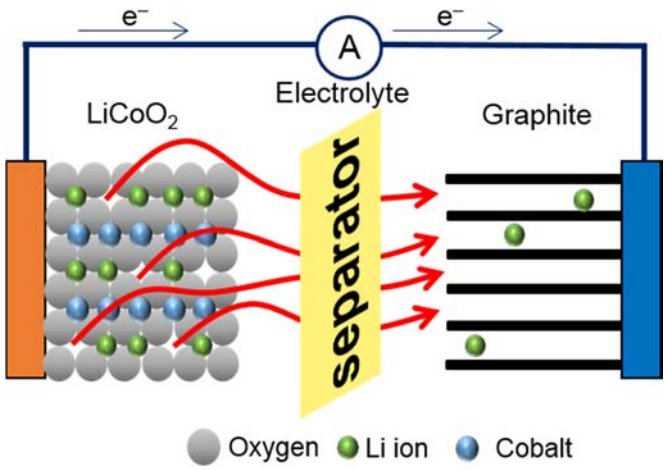

Figure. 1. Charging process Schematic of the conventional Lithium-ion batteries. Cathode is Li-ion host material and reduced ($A^+ + e^- \rightarrow A$) during discharging process of full cell: $LiCoO_2$ ⎪ Li^+ contain Electrolyte ⎪ Graphite.

1.2. Organic compounds as an active material for rechargeable batteries

(Overview of organic compounds as electrode materials)

These days, inorganic compounds have been dominated the battery market in the area of cathode. Organic compounds as electrode materials for rechargeable batteries, however, has history as long as inorganic compounds. As a matter of fact, the first commercialized primary battery that the beginning of the lithium ion batteries is lithium metal with $(CF)_n$ in non-aqueous electrolyte by Fukuda in 1973, Li │ $LiBF_4$ in GBL (γ-butyrolactone) │ $(CF)_n$.[5] After that, the interest of develop organic materials were decreased since SANYO Electric Co. commercialized lithium metal battery by using inorganic compound for LED fishing floats, cameras and memory backup applications in 1975, Li │ $LiClO_4$ in PC/DME (propylene carbonate/Dimethyl ether) │ MnO_2.

The study of organic materials was significantly reduced because of the increasing interest of inorganic material. In 1976, the inorganic materials for batteries were occupied market by using influential material, TiS_2, as cathode material for rechargeable or secondary battery by M. S. Whittingham in Exxon.[3, 6-7] J. B. Goodenough, also, reported transition metal oxide as a cathode material, $LiCoO_2$, in 1980 and the inorganic research became big and huge.

But now, Lithium as well as Magnesium[8], Zinc[9] and air[10] batteries were investigated by applying electronic equipment. As a logical alternative to the conventional cathode or anode materials, also, organic materials have attracted academic attentions from the viewpoint of (1) unlimited elemental resources and (2) elastic properties guaranteeing flexibility in case of polymeric materials. Various moieties including conducting polymers (CPs)[11-17], free radical (-NO•)[18-26], carbonyls (C=O)[27-39] and non-conjugated compounds. The properties of these various compounds were described.

1.2.1. Conducting polymers

The mechanism of the conducting polymer as an active material for battery with electrochemically doping. Cations or anions as dopant in electrolyte react with conducting polymer film as working electrode. Because of this, the capacity is determined by the number of dopant (Li^+ or anion, e.g. ClO_4^-, PF_6^-) in electrolyte. The capacity, once again, depends on its concentration of electrolyte.[40]

To increase practical capacity, size control research was attempted with poly (aniline) nanotubes and nanofibers by Jun Chen et al.[41] One of the well-known conducting polymer, Poly (aniline), PANI, is unique material because of its chemical, electrical and optical performances during oxidation/reduction.[42-44] This group synthesized perchloric acid-doped poly (aniline) ($HClO_4$-doped PANI) nanotubes by using anodic aluminum oxide (AAO) membranes and dopant, ClO_4^-, in electrolyte lithium salt $LiClO_4$.[45-48] The AAO membranes had a cylindrical pore structure with a uniform pore diameter of about 200 nm and thickness around 60 um.

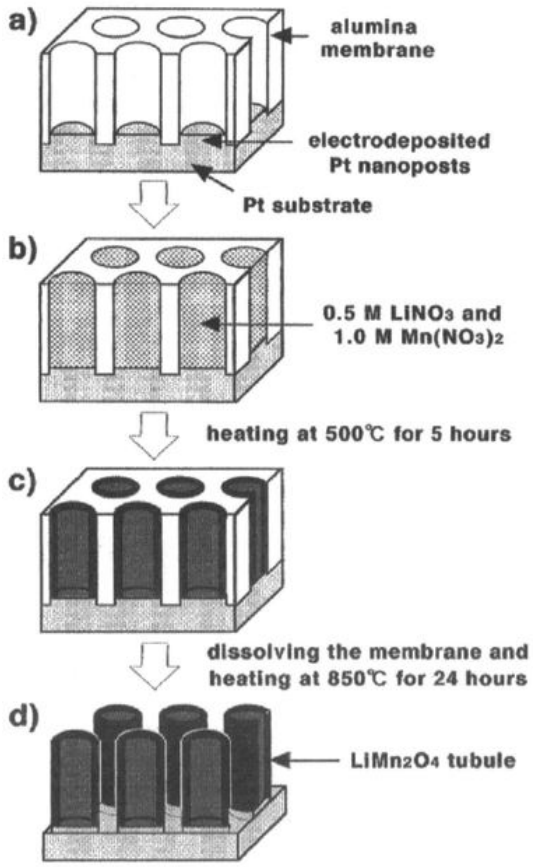

Figure. 2. The Schematic illustration of the tubule array with AAO membranes to make $LiMn_2O_2$ nanotubes.[45]

Figure 2 showed the method how to make nanotubes by using AAO membranes even though product is not our goal material. The Scanning electron microscopy (SEM) images showed morphology of $HClO_4$-PANI nanotubes (**Figure. 3**).

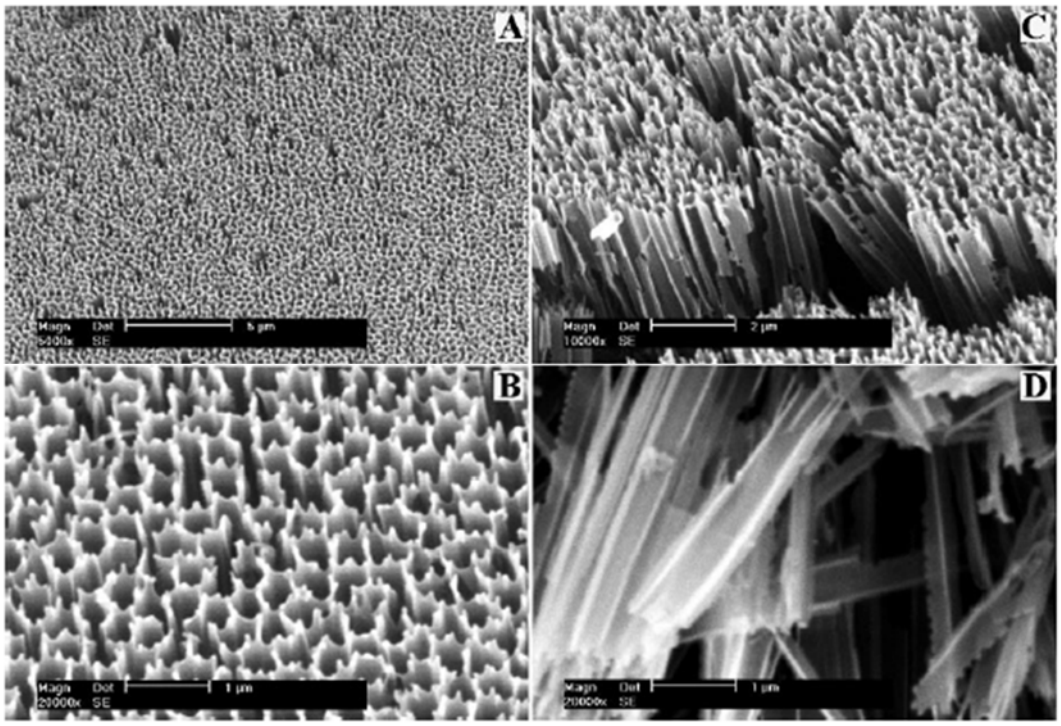

Figure. 3. SEM images of $HClO_4$-PANI nanotubes. (A, B) Overall views of the nanotubes. (C) Top view. (D) After ultrasonic treatment.[41]

The 1D nanostructure have high surface areas and possibly enable faster diffusion kinetics, it could be make good electrochemical performances. (1) Shape oxidation/reduction peaks can be identified with CVs. Increasing of the current amount with PANI nanotubes, also, confirmed and leads to capacity directly during the cyclic process **(Figure. 4).** (2) The capacity of nanotubes around 76 mAh g^{-1} with during the charge/discharge process at 20 mA g^{-1} (charged and discharged around 0.15C-rate) **(Figure. 5)**.

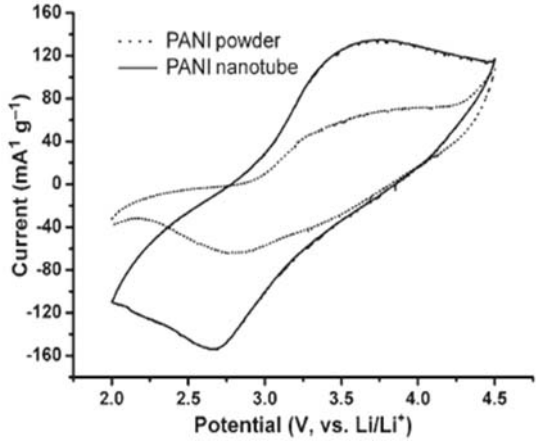

Figure. 4. Cyclic voltammograms (CV) with PANI powder and PANI nanotubes. Second cycle is shown. Scan rate= 1 mV s^{-1}. 0.5 M $LiClO_4$ dissolved in PC/DMC (1/1 wt. %) used as an electrolyte.[41]

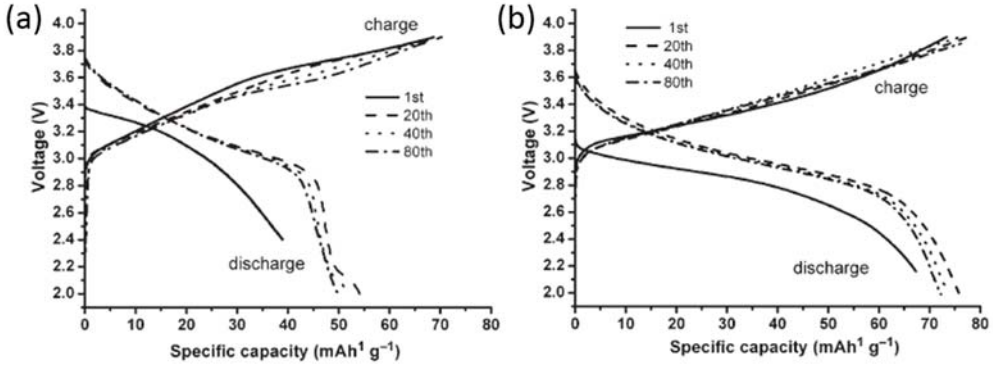

Figure. 5. Charge/discharge profiles with 20 mA $g^{-1}$with **(a)** commercial doped PANI powder and **(b)** PANI nanotubes. Potential range= 2.0 ~ 3.9 V versus Li/Li^+. The electrode was coated on the pores of the steel mesh with spray coating method by using 20 wt. % of $HClO_4$-PANI in N-Methyl-2-pyrrolidone (NMP) solvent.[41]

Figure 4 and 5 were evaluated the performances of PANI nanotubes as a good electrochemical equipment for rechargeable batteries with commercial powder as a comparison. Nanostructure features befitting fast charge/discharge rate is expected to show a good performances.

1.2.2. Free radical compounds

Nitroxide radical compounds contain the N-O bond with one unpaired electron delocalized. The mechanism of radial compounds during the oxidation (charge)/ reduction (discharge) is like as **Scheme 1**. One unpaired electron or radical compounds is known to initiate and propagated polymerization and combustion reactions with their high reactivity.

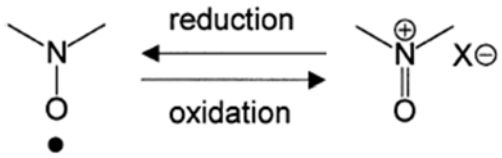

Scheme. 1. Oxidation and reduction mechanism of radical compounds. A dot symbolize an unpaired electron.

Electrochemical studies of nitroxide radical compounds presented reversible redox reaction with one electron oxidation from nitroxide radical to oxoammonium cation and reduction to original state of the compound. This reversible oxidation of radical compounds is used as p-type doping. While a phenoxyl radical is one electron reduced to form a phenolate anion and is used as n-type doping. Also these radical compounds, nitroxide and phenoxyl radical, belong to cathode and anode material, respectively.

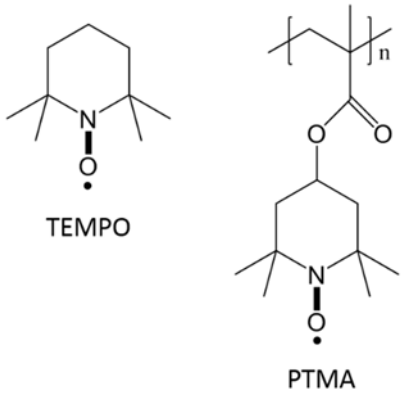

Figure. 6. Structure of TEMPO and PTMA.

To discuss an example of the active materials for batteries utilizing the redox mechanism, one of the most well-known radical material was used, 2,2,6,6-Tetramethylpiperidin-1-oxyl (TEMPO). [49] TEMPO was synthesized by radical polymerization and acted fast initiator to contribute chains.[50] In 2002, Nakahara et al. reported poly (2,2,6,6-tetramethylpiperidinyloxy methacrylate) (PTMA) organic radical cathode material (**Figure. 6**).[21]

The oxoammonium cation which is oxidized form of the TEMPO was isolated under ambient conditions. Chemical stability of nitroxide and oxidized form of nitroxide is important during the charge and discharge process of the batteries. In the form of nitroxide, the N-O bond was found 1469 cm^{-1} FT-IR peak and had 1.28 Å length. In the case of oxidized form of nitroxide, or oxoammonium cation, has 1626 cm^{-1} IR peak and 1.18 Å chain length. The process from reduced species to oxidized species was very slight which could be for the facile electron transfer reaction of the radical compounds batteries (**Scheme. 2**).[51-52]

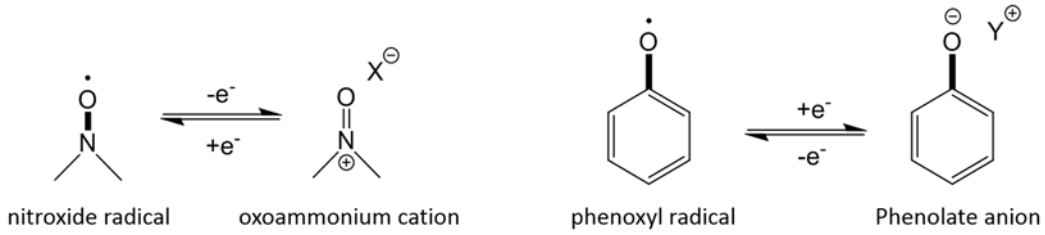

Scheme. 2. oxidation/reduction mechanisms of nitroxide and phenoxyl radical compounds.[51]

Electron transfer rate constant (κ_o) of nitroxide radical and phenoxyl radical were revealed on the order of 10^{-1} cm s^{-1}. That values are even higher than that of for ferrocene (10^{-2}) which well known as a standard molecule in electrochemical activity and similar with copper ion (Cu^{+}), ~10^{-1}.[51] Big difference in terms of electron transfer rate were checked when compare with the disulfide compound which is a kind of organic active material. This is evidence to inform ensures facile electron transfer rate of the radial compounds. They investigated electrochemical properties with CV in diffusion limited system. PTMA was mixed with graphite and binding powder as a working electrode (1/8/1 wt. %). Li/Li+ and platinum wire were used as a reference and counter electrode, respectively. 1 M $LiPF_6$ in ethylene carbonate (EC)/ diethyl carbonate (DEC) (3/7 wt. %) was used as an electrolyte. The half potential ($E_{1/2}$) of PTMA is around 3.58 V and separation of the oxidation and reduction peak is about 0.16 V (peak of oxidation= 3.66 V, peak of reduction= 3.5 V). The small gap of the oxidation and reduction peaks agrees with the electrode could be operate with fast charge transfer, especially works nicely when tested fast charge/discharge C-rate (**Figure. 7**).

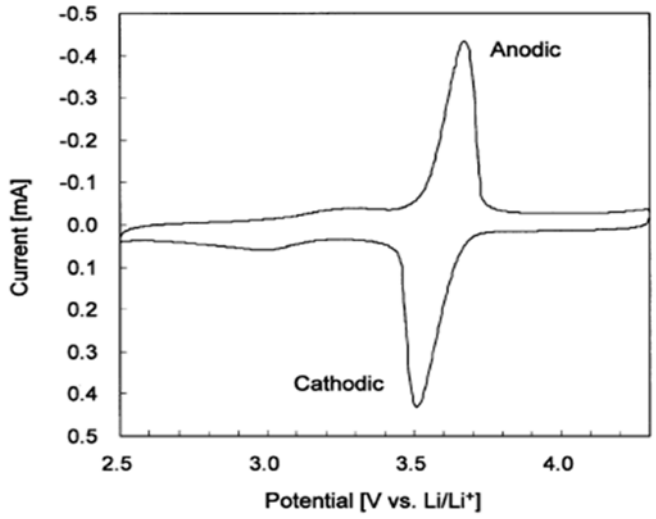

Figure. 7. CV of electrode with PTMA as an active material. Scan rate= 10 mV s^{-1}.

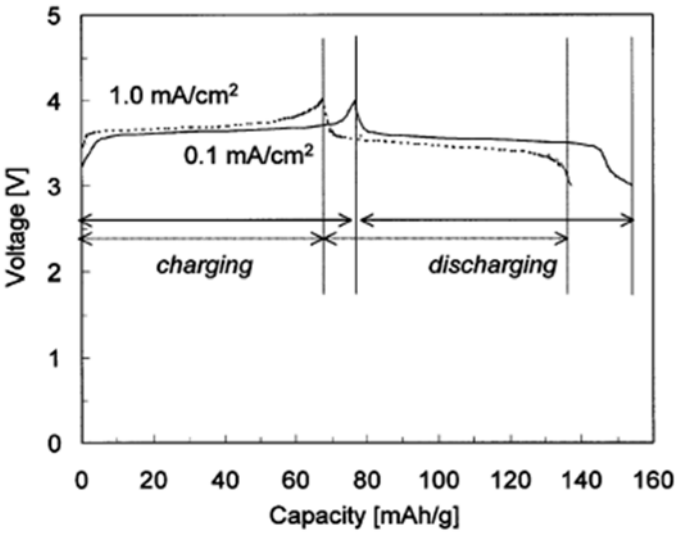

Figure. 8. Charge/discharge profiles for PTMA as an active material with 0.1 mA cm^{-2} and 1.0 mA cm^{-2} current density.

The charge/discharge cell test was activated with PTMA, graphite and binder (1/8/1 wt. %) as a working electrode. The experiment was conducted with two types depending on the current density, 0.1 mA cm^{-2} (1.2C) and 1.0 mA cm^{-2} (12C). The working potential is between 3.0 V and 4.0 V and plateau potential is nearly 3.5 V. The theoretical capacity of PTMA is 111 mAh g^{-1} in only one electron transfer system and initial capacity during discharge is around 77 mAh g^{-1} at 0.1 mA cm^{-2}. 70 % of theoretical capacity was given on its capacity experimentally, it seemed not so wonderful

material for rechargeable batteries. In terms of charge transfer rate, however, was fast. At high current density (1.0 mA cm^{-2}), the discharge capacity was nearly 91 % of theoretical capacity. In other words, high current density gave more effective electrochemically performances and electron transfer rate of the electrode was facile reaction (**Figure. 8**).

To make advanced PTMA electrode for batteries, the effect of the CNT was reported by Nishide and Geckeler research group in 2011.[53] They informed performances of PTMA for the rechargeable batteries earlier and they tried to more advanced organic electrodes. To more stable and best performance electrode, a system that can be utilized the interaction of Single-walled carbon nanotubes (SWNTs) and PTMA composite electrode were figured out. Polymer, PTMA, wrapping could be one of the best method for SWNTs with redox active material. Through the SWNTs network with PTMA, the electrode exhibited high electrical conductivity and prominently high rate capability with nanocomposite. They discovered nanotubes were available relatively strong interactions, such as covalent bonding, π- π interactions and π-cation interactions.[54-56] The morphology of PTMA wrapped SWNTs was confirmed by Transmission electron microscopy (TEM) images (**Figure. 9**).

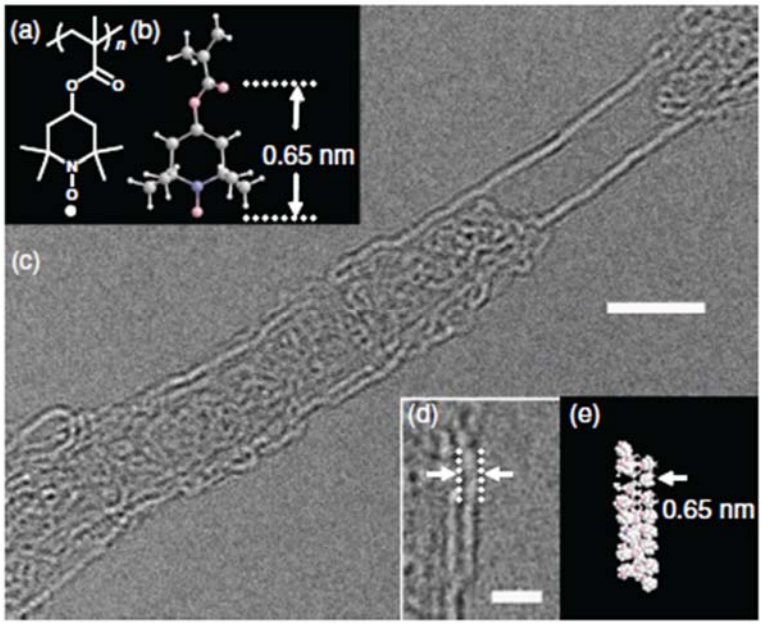

Figure. 9. (a, b) Structure and X-ray crystal structure of PTMA. **(c, d)** Transmission electron microscopy (TEM) images of PTMA wrapped SWNTs. **(e)** Space filling model of PTMA with molecular calculations.[53]

The charge/discharge curves were displayed with various current density from 1 A g^{-1} to 60 A g^{-1}. A plateau potential of PTMA wrapped SWNTs was pretty high around 0.8 V vs. Ag/AgCl which was 4.0 V vs. Li/Li^{+}. The Coulombic efficient was found 93 % and nearly 100 mAh g^{-1} capacity was displayed

with PTMA/SWNT composite electrode at 1 A g^{-1}. The value was similar to the theoretical capacity (~111 mAh g^{-1}) and showed better performances than pristine PTMA electrode (**Figure. 10**).
Reported research said that carbon nanotube not only increased capacity quantitatively and has excellent performance at high C-rate. The reason of the phenomena was the facile electron transfer by interaction between active material and nanotubes.

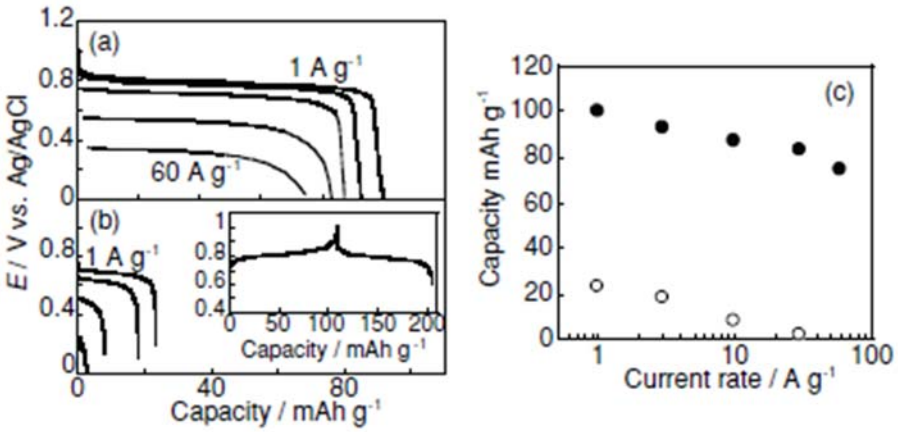

Figure. 10. Discharge curves with (a) PTMA/SWNT (4 wt. %) and (b) only PTMA cells, inset: charge/discharge curves of the PTMA/SWNT composite electrode with 1 A g^{-1} in acetonitrile containing 0.1 M $TBAClO_4$. (c) The PTMA/SWNT (black circle) and PTMA (white circle) composite electrodes capacity during discharge processes.[53]

1.2.3. Carbonyl compounds

Organic carbonyl compounds (C=O) are common materials that can be good ability of oxidation with oxygen non-paired electrons. The compounds as active material for the batteries has have been studied for a long time. The mechanism of the charge/discharge reaction with carbonyl compounds is the same as the **scheme 3**.

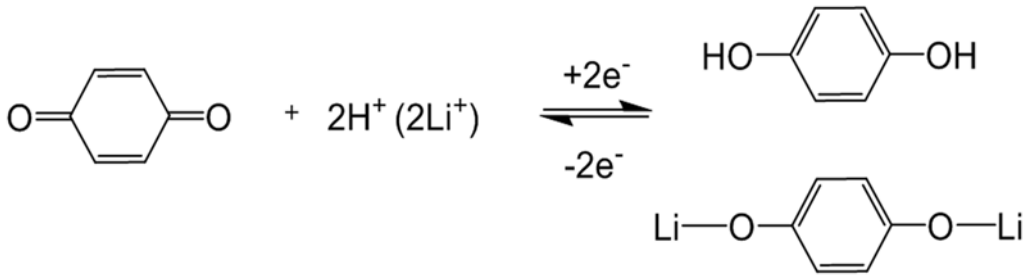

Scheme. 3. Oxidation/reduction of carbonyl compounds (C=O), basically.

In 1969, dichloroisocyanuric acid (DCA) was used as an organic cathode material for primary battery in organic non-aqueous electrolyte by Williams research group.[29] The composition of the working electrode; DCA: carbon black: carbon fibers= 83: 16: 1. No binder system was applied and two step reaction, 3.5 V and 3.0 V, was observed despite three carbonyl groups contained material (**Figure. 11**). The use of the latest analysis electrochemically, however, some good performance could be gained.

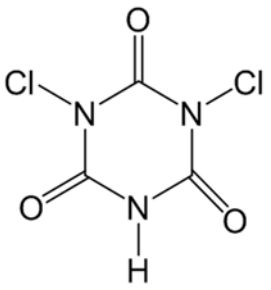

Dichloroisocyanuric acid (DCA)

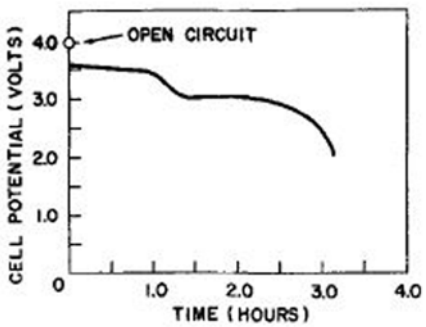

Figure. 11. Structure and discharge profile of DCA as an active material with two step reaction.

Carbonyl group was used for the beginning secondary, or rechargeable, battery in 1972.[57] Alt research group investigated mainly chloranil which has high theoretical capacity, ~ 218 mAh g^{-1} with two electron transfer system. The electrochemical tests were exhibited with various organic electrolyte and they tried to found an appropriate electrolyte with active material. All electrochemical tests were proceed with half-cells, composition of the working electrode with active material and graphitized carbon in a weight ratio of 1:1 and mixed in a ball mill for 16 hours. A saturated calomel electrode (SCE) and graphite were acted as a reference and counter electrode. (1) 3M H_2SO_4 electrolyte system of the half-cell was tested. The reversibility of the electrochemical oxidation/reduction were confirmed with CV. The half potential ($E_{1/2}$) of Chloranil in dilute sulphuric acid electrolyte was around 0.7 V versus SCE (0.241 V vs. standard hydrogen electrode (SHE)) and separation of the oxidation/reduction peak was exposed about 0.15 V (peak of oxidation= 0.75 V, peak of reduction= 0.6 V). ($E_{1/2}$= 3.941 V vs. Li/Li^+) Charge and discharge processes were confirmed by galvanostatically test. The practical capacity decreased slightly with increasing of current density, C-rate (**Figure. 12 and 13**).

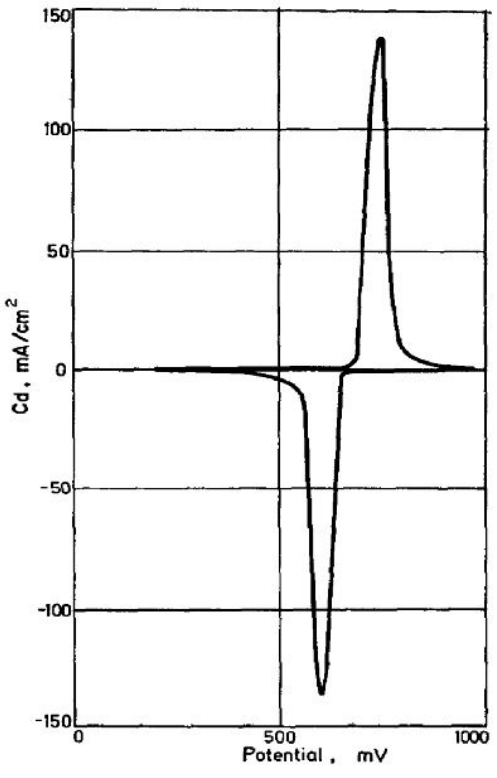

Figure. 12. CV of chloranil as an active material in the system of dilute sulphuric acid. Scan rate= 0.33 mV s^{-1}.

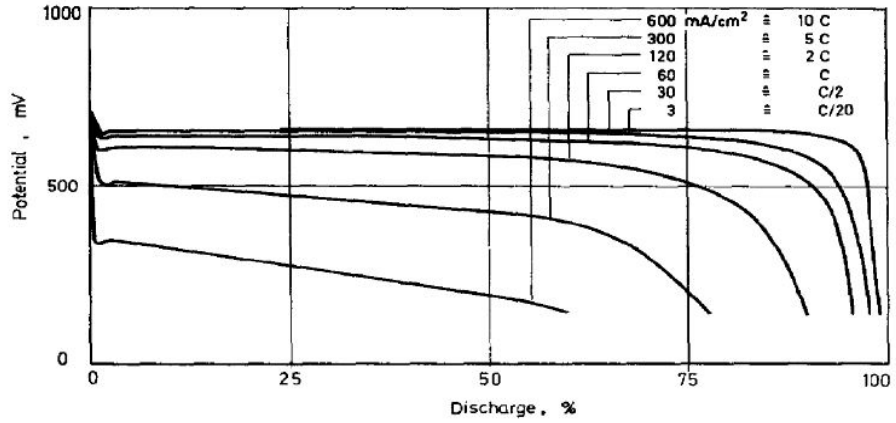

Figure. 13. Discharge curves of chloranil in dilute sulphuric acid with diverse C-rate. (Potential vs. SCE)

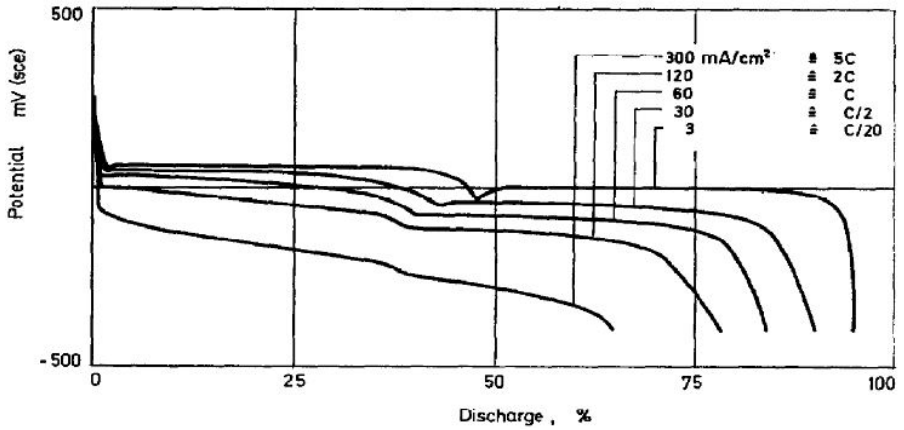

Figure. 14. Discharge curves of chloranil in ammonium chloride solution with diverse C-rate. (Potential vs. SCE)

(2) 5 M NH_4Cl solution activity of chloranil had difference performances with sulphuric acid solution. It came into existence two peaks during the oxidation and reduction and aslo negative potential shifts were observed, $E_{1/2}$= 3.291 V vs. Li/Li^+. (Sulphuric acid electrolyte, $E_{1/2}$= 3.941 V vs. Li/Li^+). Two peak separation was 70 mV and those two charge transfer reactions were facile reaction (**Figure. 14 and 15**).

They measured the electrolyte dependence behavior of a chloranil working electrode and it may be assumed that the selection of the electrolyte is important in the case of low molecular weight organic active material.

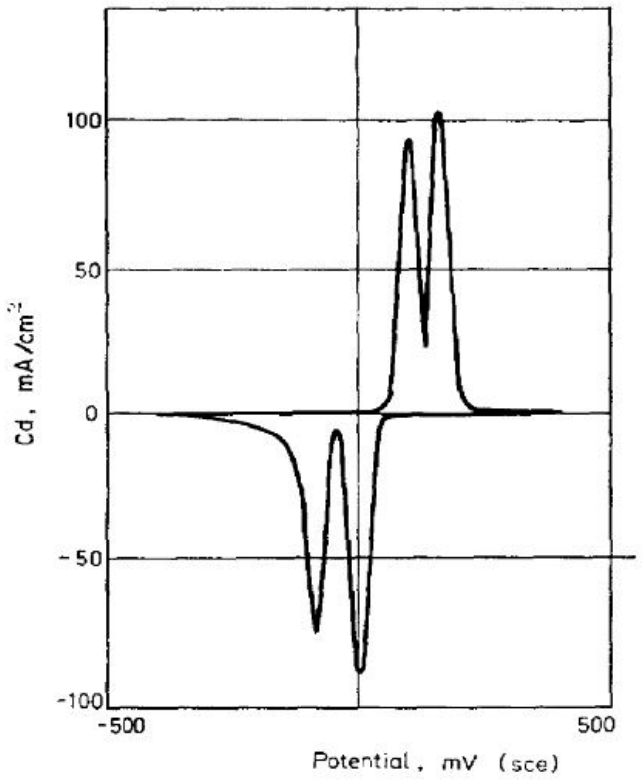

Figure. 15. CV of chloranil as an active material in the system of ammonium chloride electrolyte. Scan rate= 0.33 mV s^{-1}.

To solve origin problems of small molecules which is the noteworthy solubility in the electrolyte, researchers have been attempted various tests. The beginning attempt was applied polymerized compounds resulted in not only reduced possibility to soluble in electrolyte, but enhanced stability during the oxidation/reduction. Polyquinone (PQ) was synthesized by J. S. Foos group in 1986 to solve the origin problems (**Scheme. 4 and 5**).[37]

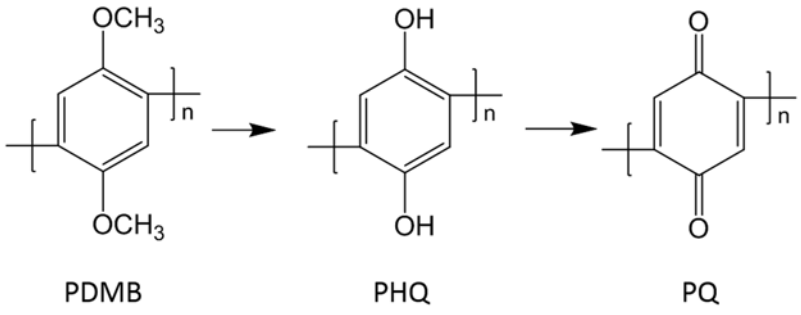

Scheme. 4. Schematics of synthesized PQ by using poly-hydroquinone (PHQ) which is anodic oxidized form of poly-1, 4-dimethozxybenzene (PDMB).

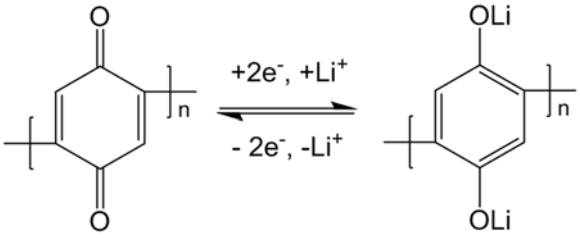

Scheme. 5. Charge/discharge mechanism of PQ.

Processes of synthesized intermediate material and final product were performed through the CV in the solution chemistry. The PDMB films were formed on the Stainless steel electrode using a constant current that was increased over the period of 4 of 5 hours to 0.4 A (~ 2.6 mA cm^{-2}) (**Figure. 16**).

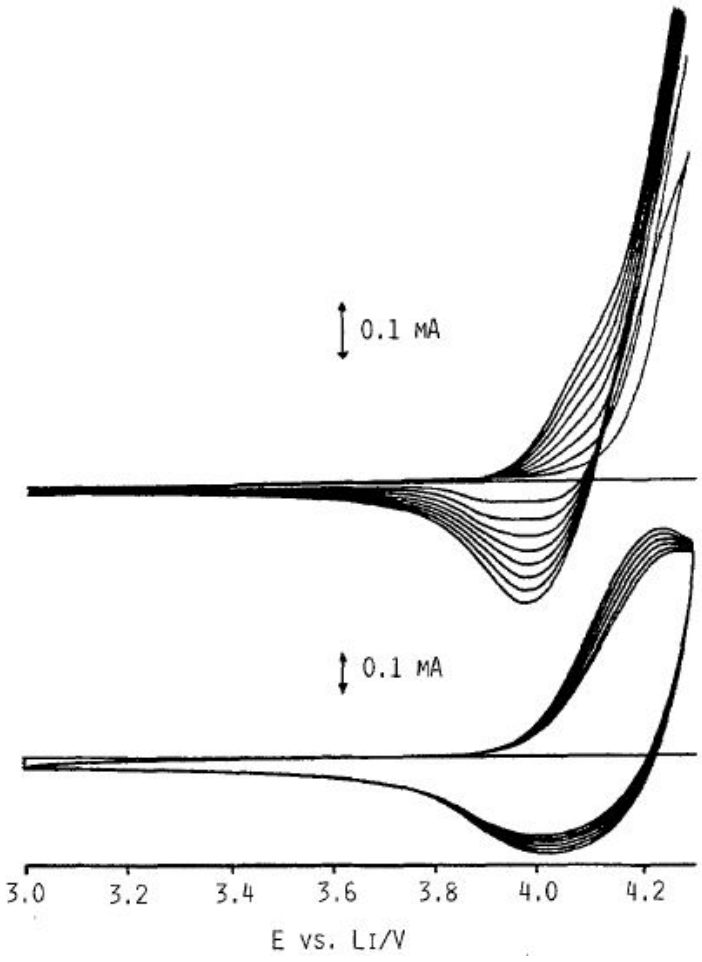

Figure. 16. Top; The creation of polymeric 1, 4-dimethozxybenzene (DMB) from DMB. Bottom; The oxidation and reduction reaction of PDMB film on stainless steel electrode. Then, filtered and washed with acetonitrile to remove PDMB from the electrode. Li metal as a counter and reference electrode. 0.5 M $LiClO_4$ in PC containing excess DMB was used as an electrolyte. Scan rate= 50 mV s^{-1}.

The PHQ acted initiator of PDMB with constant heat-treatment 130 ~ 140 ^oC for 24h under argon gas. And it can be confirmed decreasing of PDMB IR peak on real time, O-CH_3 (1035 cm^{-1}) by monitoring. The PQ/carbon and Teflon (8/2 wt. %) were physically mixed on 1.3 cm diameter of Ni steel die as a working electrode around 1.2 g/ cm^3 and Li counter electrode were used. $LiClO_4$ in propylene (PC) or $LiAsF_6$ in tetrahydrofuran (THF) was acted electrolyte in the cells (**Figure. 17**).

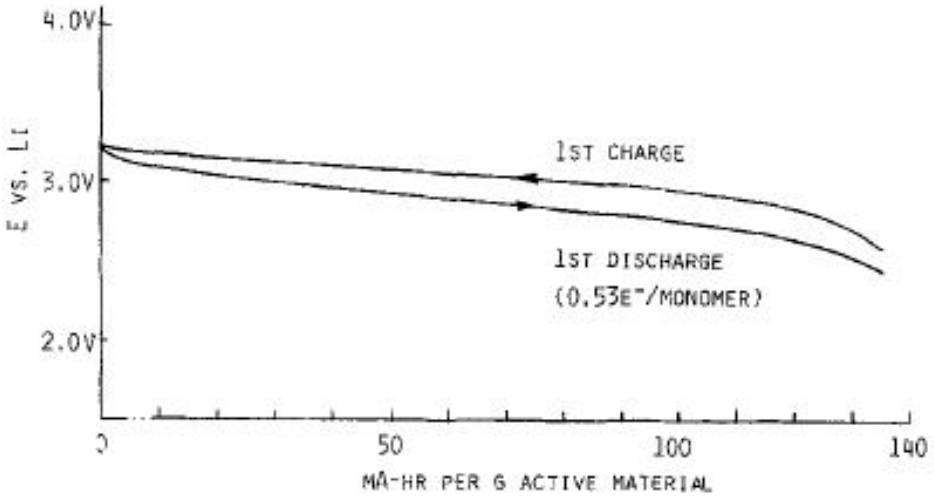

Figure. 17. The first cycle profiles of PQ with carbon in $LiAsF_6$ in THF electrolyte.

In 1986, Pasquali research group experimented organic material with having unlimited capacity which is one of valuable advantage of organic active material. To make extremely high performance battery in terms of capacity, Nonylbenzo-hexaquinone (NBHQ) which has huge theoretical capacity as 489 mAh g^{-1} investigated with large planar structure to prevent dissolution at electrolyte.[58] In the process, only a quarter of the theoretical capacity was not implemented. There was an expectation of practical capacity; some of the electrons were used to generate radical anions, so the number of active electron decreased as shown in **figure 18.**

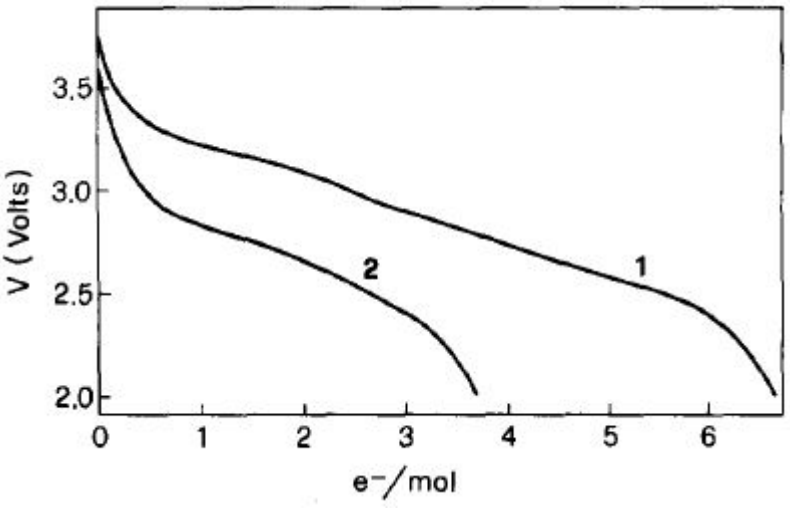

Figure. 18. The first and second discharge curves at 0.1 mA cm^2.

A cell was discharged at low rate (0.1 mA cm^2) in order to find the number of electrons involved in the observed CV. At the first discharge, 7 electrons were participated in the reaction while 4 electrons involved in reaction at the second discharge. 3 electrons were used which generated radical anions during the reduction. The reaction schemes were based on the evidence during the reduction;

(a) $NBHQ + 3e^- + 3Li^+ \rightarrow (NBHQ)^{3-\bullet}3Li^+$

(b) $(NBHQ)^{3-\bullet}3Li^+ + 4e^- + 4Li^+ \rightarrow (NBHQ)^{3-\bullet}3Li + (NBHQ)^{-4}4Li^+$

To more additional information, the basis study of anthraquinone by CV with 50 wt. % teflonized acetylene black as a binder and conducting agents. Even it is hard to say the potential is appropriate to cathode or anode for batteries, the compound showed clear single peak at 2.3 V vs. Li/Li^+ (**Figure. 19**). The discharge curves of NBHQ were tested with 0.5C-rate and the cell showed capacity around 120 mAh g^{-1} over the 500 cycles (**Figure. 20**).

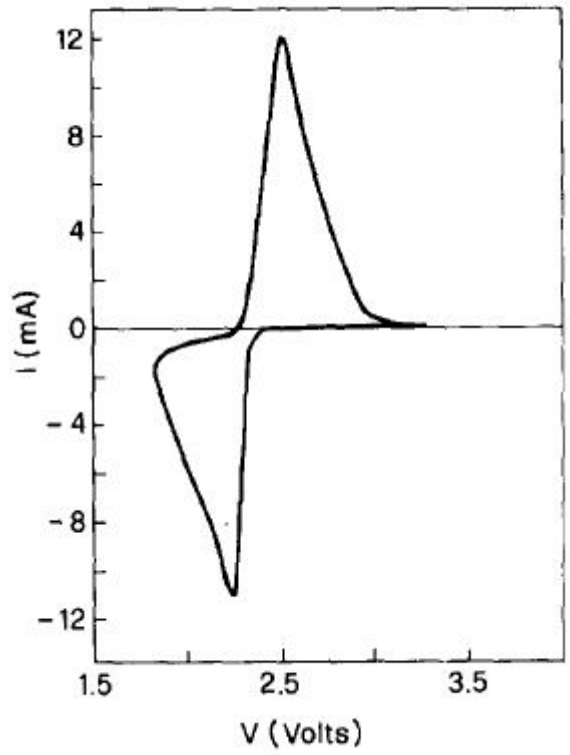

Figure. 19. CV with basic material, anthraquinone, of NBHQ. Scan rate= 1 mV s^{-1}. Electrolyte= $LiClO_4$ in PC/DME (1/3 wt. %).

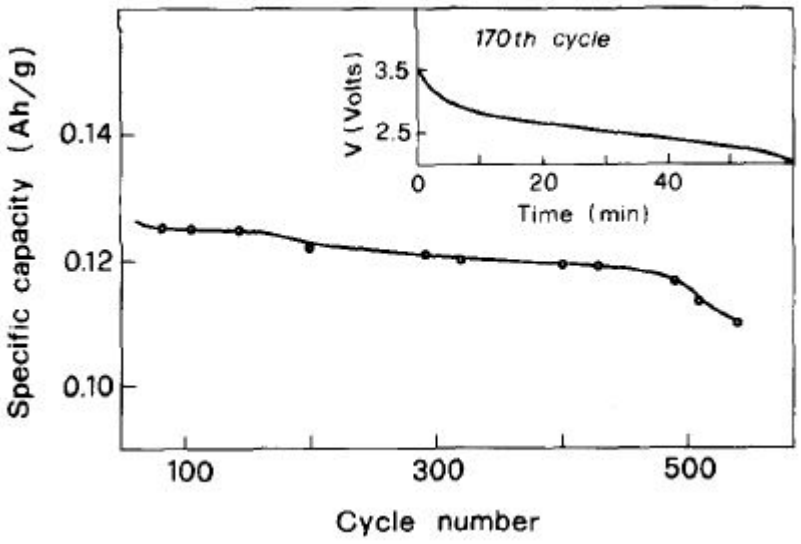

Figure. 20. Discharge capacity of NBHQ electrochemical cell at 0.5C during over 500 cycles. Inset figure showed a representative discharge profile.

Charge and discharge electrochemical cell test of NBHQ was performed with 50 % teflonized acetylene black (acetylene black/ Teflon, 3/1 wt. %) at 0.5C charge and discharge rate. Around 125 mAh g^{-1} capacities were observed and also the cell had brilliant stability in the organic half-cell, $LiClO_4$ in PC/DME (1/3 wt. %). Despite the good stability performances, practically low working potential (2.6V vs. Li/Li^+) and low capacity (only 25 % of theoretical capacity was obtained) were revealed.

At 1999, Haas group developed advanced electrochemical cells by using conducting polymer complex with carbonyl contained compound. The electrode material contributed high electron or ion transfer rate during the charge and discharge. Active sites in carbonyl structure into polyaniline (PANI) conducting polymer backbone, poly (5-amino-1,4-naphthoquinone); PANQ, and two electron were reacted with lithium ions which are main conductor in LIBs. 0.75 M $LiClO_4$ in acetonitrile was used electrochemical cell solution. Cathode composite electrode consisted of PANQ, oppanol binder and carbon black (49/2/49 wt. %). Even the working potential, 2.6 V vs. Li/Li^+, was ambiguous, the practical capacity (second discharge capacity= ~250 mAh g^{-1} at 1C-rate) was similar to theoretical capacity (290 mAh g^{-1}). The overall insertion and de-insertion of Li-ions into or from PANQ working electrode followed three steps; (1) diffusion of Li-ions between PANQ and carbon grains in the liquid electrolyte, (2) oxidation and reduction in PANQ or at the surface of PANQ electrode, (3) diffusion of Li-ions in the bulk of the polymer. Further examinations are needed, however, to determine capacity loss during the first and second cycling.[32] The group of poly aminonaphoquinones showed good conductivities at both oxidized and reduced species, ~10^{-3} to 10^{-1} S cm^{-1}.[59-60]

1.3. Poly vinyl carbazole (PVK)

Poly (N-vinyl carbazole) (PVK) which is made from polyvinyl alcohol and having large side chain based on N-containing heterocyclic ring carbazole group (**scheme. 6**) has been used as organic photoconductor in the area of photoconductive and photosensitive devices.[61-62] High frequency electrical properties and photoconductive properties have been applied to a high frequency insulation material, copier drum transport layer and holography's photosensitive material. Therefore, it can be a photoconductor. PVK can dissolved in series of non-polar solvent such as ethyl acetate, acetone, benzene, toluene, xylene, tetrahydrofuran and concentrated nitric acid, which does not soluble in alcohol, ether, aliphatic hydrocarbon and acid.

There are many particular properties except for photoconductive: (1) Thermoplastic, polymer that becomes pliable or moldable above a specific temperature and returns to a solid state upon cooling. Also, vinyl-based polymer having weak intermolecular interactions of the thermoplastic characteristics. (2) Resistant to acid, alkali, dilute HF. (3) Mica and asbestos substitution. (4) Softening point of 220 ^{o}C, 310 ^{o}C decomposition. (5) High heat, water- resistance and chemical stability. (6) Good brittleness and elongation.

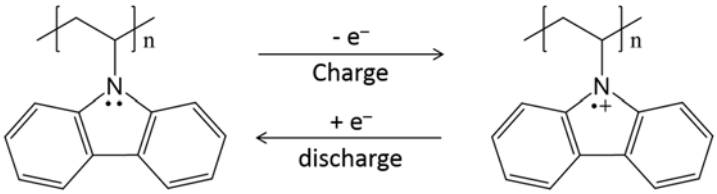

Scheme. 6. Mechanism of PVK during the charge (oxidation) and discharge (reduction) processes in the battery system.[63]

- Poly (9-vinylcarbazole)
- Formula= $(C_{14}H_{11}N)_n$
- Average Mn= 25,000 ~ 50,000
- Melting point= 300 ^{o}C
- Color= White, light yellow
- Sigma-Aldrich, 368350

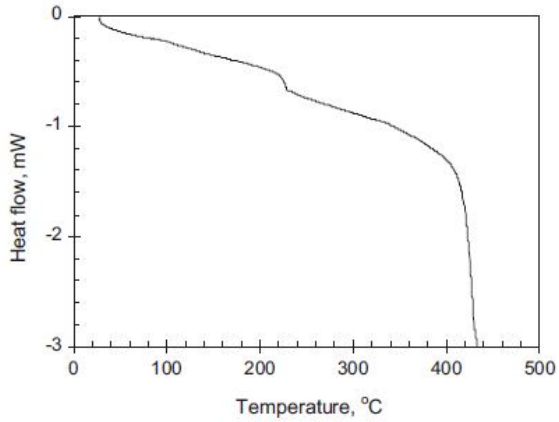

Figure. 21. Thermal stability of PVK tested by Differential scanning calorimetry (DSC) under a hydrogen atmosphere. Heating rate= 10 ºC min^{-1}.[63]

In my study, PVK was used as a cathode material for rechargeable batteries. Its electronic pathway is designed by the π-stacked structure of the carbazole moiety in the polymer. In addition, a redox potential exists over 4 V vs. Li/Li^+.[64-66] Thermal stability of PVK was tested by Differential scanning calorimetry (DSC) [63] and PVK showed an endothermic demeanor at around 400 ºC to decomposition (**Figure. 21**). In contrast with the $LiCoO_2$, PVK endothermic reactions have good thermal stability.[67] Nowadays safety of the battery have been emphasized, PVK considered as a single countermeasure for a wide temperature range rechargeable batteries. Also, Yao et al. researchers applied PVK as a binder with $LiFePO_4$ which is well known cathode material. Although the composite electrode was slow to react between $LiFePO_4$ and PVK electrochemically and PVK when compared with the PVdF conventional binder had outstanding electrochemical performance.[63] Increased 9 percent of practical capacity (150 mAh g^{-1} with PVK binder, 138 mAh g^{-1} with PVdF binder at 0.25C charge/discharge rate) and better cycle stability were performed.

1.4. Inter-tangled polymers: PVK and PEDOT:PSS

Most of conducting polymers are p-type conductors in which positive charge carriers called sometimes polarons move within or between polymeric backbones.[68-70] Only oxidized state of conducting polymers is electrically conductive. Anionic dopants neutralize the positive charges of conducting polymers in their oxidized state. At potentials negative enough to reduce conducting polymers, they turn into semi-conductors or insulators, losing positive charges as well as dopants (in case of small-molecular anions such as Cl^-). Dopants are required in conducting polymers. Positive charges were developed during synthesis of the conducting polymers, which play a role of charge carriers through polymer backbones for conduction. PSS is the dopants of PEDOT so that sulfonate groups neutralized the positive charges of conductive PEDOT.

PEDOT:PSS (Poly(3,4-ethylenedioxythiophene) doped with poly(styrenesulfonate)) as a representative conducting polymers shows very high conductivity up to higher than 3,000 S cm^{-1}.[71] Its reduction potential is -0.2 V to -0.5 V versus Ag/AgCl in aqueous electrolyte (equivalent to +2.8 V to +2.5 V versus Li/Li^+; shifted to more negative vales in organic electrolytes as discussed below). Since conducting polymers are also redox-active, the values of their reduction potentials should be compared with those of redox-active polymers when composite electrodes of them are made. The reduction potential of PVK is more positive than that of PEDOT:PSS so that there is a possibility of electron transfer from PEDOT:PSS to PVK. At an initial condition just after electrochemical cells are made, however, such an electron transfer is not allowed because PVK and PEDOT:PSS are already in their reduced and oxidized states, respectively. There are no room where extra electrons are gained in PVK while PEDOT:PSS does not have extra electrons that can be donated. Similar situations are expected at potentials more positive or negative than reduction potentials of both PVK and PEDOT:PSS.

To materialize an ideal model system in which a redox-active polymers as an active material is tangled with a conducting polymer providing electric pathways, a composite architecture of PVK and PEDOT:PSS was developed as an anode of LIBs. No additional binders were used because PEDOT:PSS plays a role of binders. As expected, performances at high rates were impressively enhanced with PEDOT:PSS when compared with a conventional binder system based on PVdF.

II. EXPERIMENT

2.1. Cell preparation

2.1.1. Influence of secondary conducting agent and dispersion solution

Composite electrodes were prepared with three classes. A working electrode composed with active material, binder, carbon black as a conductive agent and carbon nanotubes (CNTs) as a secondary conducting agent. Polyvinylidene fluoride (PVdF) or polyacrylic acid-carboxymethyl cellulose (PAA-CMC) was used as binder. A mixture of polyvinyl carbazole (PVK) as an active material, carbon black as a conductive agent and CNTs were blended with PVdF dissolved in N-Methyl-2-pyrrolidone (NMP). In contrast, PVK, carbon black and CNTs were blended with PAA-CMC dispersed in water. The slurries with a viscosity similar to honey were pasted on aluminum foils by using a doctor blade coater. The thickness of doctor blade coater was controlled by 300 um. The composite electrodes were dried at 60 ^{o}C overnight. The water-based composite electrode was additionally dried under vacuum at 120 ^{o}C for 2 hours to remove water totally (**Table 1**).

2.1.2. Conductive binder PEDOT for composite electrode

Aqueous solution of 1.3 wt. % PEDOT:PSS (Poly (3,4-ethylenedioxythiophene) doped with poly(styrenesulfonate)) was mixed with carbon black dispersed solution of PVK in NMP. The well mixed slurry was pasted on aluminum foil by using a doctor blade, 300um. The electrode was dried at 60 ^{o}C overnight and under vacuum at 120 ^{o}C for 2h.

2032-coin type half cells were organized by working electrode and lithium metal as a counter and reference electrodes. Separator was located between working and counter electrodes. 1 M $LiPF_6$ in ethylene carbonate/dimethyl carbonate (1:1 v/v, EC/DMC) was appropriate for an electrolyte for all cells (**Appendix. 6. 1**).[72]

Table. 1. Typical compositions of composite electrodes.

Group	Weight ratio
PVdF	PVK : PVdF : carbon black = 5 : 1 : 4
PVdF + CNTs	PVK : PVdF : carbon black : CNTs = 5 : 1 : 2 : 2
PAA-CMC + CNTs	PVK : PAA-CMC : carbon black : CNTs = 5 : 1 : 2 : 2
10 % PVdF	PVK : PVdF : carbon black = 5 : 1 : 4
1 % PEDOT	PVK : PEDOT:PSS : carbon black = 5 : 0.1 : 4

PVK (Sigma 368350, MW=25,000~50,000), PVdF (Solvay, Solef 5130), PAA-CMC (1:1, % of PAA: % CMC, Sigma-Aldrich 323667), PEDOT:PSS (Poly(3,4-ethylenedioxythiophene) doped with poly(styrene-sulfonate)) (Heraeus, Clevios PH1000, 1.0~1.3 wt.% aqueous solution), Carbon black= Super P (TIMCAL), CNTs (Thin multi wall CNT, NANO Solution TMC 110920-11)

2.2. Electrochemical analysis

Cyclic voltammograms (CV) and electrochemical impedance spectroscopies (EIS) of cells were observed with a potentiostat (Biologic, VMP3). Cells were galvanostatically cycled between 2.0 V and 4.7 V versus Li/Li^+ without a potentiostatic period by using a battery tester (WonATech. WBCS3000). The current for 1C-rate was defined as 120 mA g^{-1} based on active material mass, PVK. Electrical conductivities of these electrodes were measured by four-point-probe technique (Dasol, Rs8-1G). The same composite slurry used in electrochemical cells were pasted on glass substrates for the conductivity measurements. Thickness of the pasted film was measured by vernier caliper.

2.3. Physical properties

Surface morphology of composite electrodes were examined by scanning electron microscope (SEM; Hitachi, S-4800). Tangling states of PVK, PEDOT:PSS and their mixture were obtained by transmission electron microscope (TEM; JEOL, JEM-2100F).

III. RESULTS & DISCUSSION

3.1. Influence of secondary conducting agent and dispersion solution

3.1.1. PVK as an active material with CNTs as a secondary conducting agent

Electric conductivity of CNTs be similar to copper (Cu) and CNTs have good thermal conductivity comparable to the diamond which is the most distinguished material. Also, it is 100 times greater than steel in terms of intensity properties.[73] In addition, CNTs could be suitable to portable electronic devices following trend and used to flexible energy devices[74].

In our works, CNTs behave supplement to improve electrochemical or mechanical performance: (1) increasing electronic conductivity (2) growing binding force with current collector. Polymer, e.g. PVK, has long carbon chain which is oxidation/reduction reaction during the charge/discharge in the battery system. The polymer wrapping carbon nanotubes while mixing paste (or slurry: active material, binder and conducting agent) and the structure of the mixture secures electron pathway. It performed high electron transfer rate and proved by electrochemical methods. 1) To investigate electrochemical properties, cyclic voltammograms, impedance spectroscopies and electronic conductivities were studied.

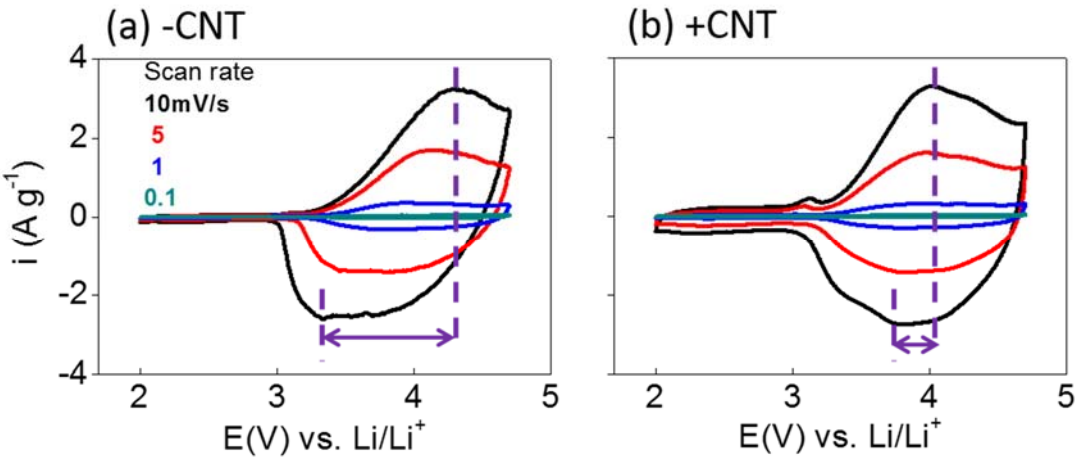

Figure. 22. The cyclic voltammograms of CNT effect with variable scan rates (10, 5, 1, 0.1 mV/s).

The gap between maximum current potential and minimum current potential indicated the kinetics that rapidity of electron transfer. Electrochemical cell with CNTs showed small potential gap that means fast

charge transfer or fast kinetics system **(Figure. 22)** with similar condition **scheme 7**. CNTs-containing composite electrode showed lower resistance regarding charge transfer between paste and current collector during the charge/discharge progressions.

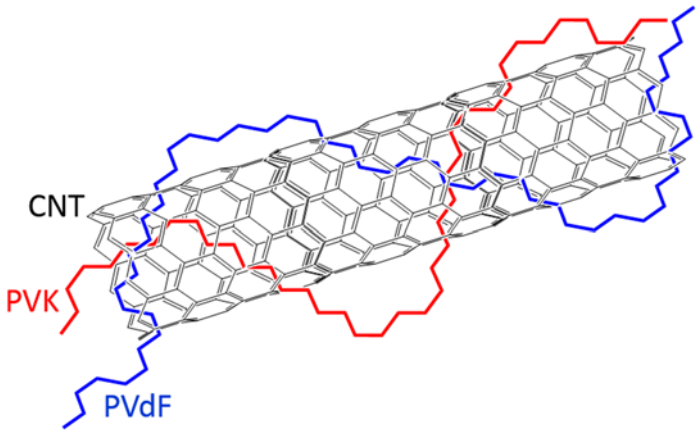

Scheme. 7. Expected schematic illustration of inter-tangled with PVK, PEDOT and CNTs (Black line: CNTs, Red: PVK, Blue: PVdF).

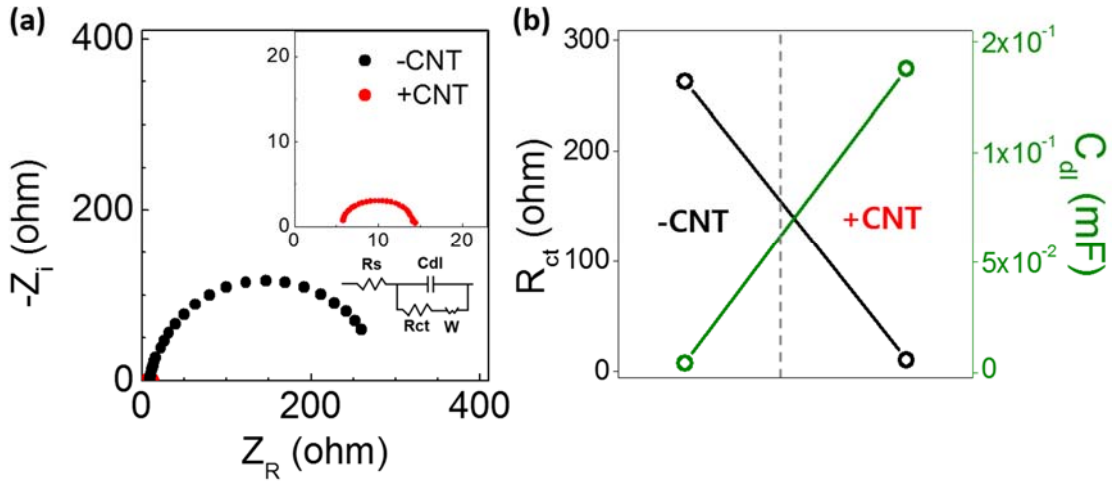

Figure. 23. (a) Electrochemical impedance spectroscopies at peak potentials 4.2 V (vs. Li/Li^+) from 200 kHz to 0.1 Hz. All cells were measured coin-type cells. **(b)** Values are calculated by fitting program, Z view.

The **figure 23** semi-circles indicate that electrolyte (R_S) and charge transfer (R_{CT}) resistances. The resistance of charge transfer with CNTs (R_{CT}^{+CNTs}= 10.93 ohm) relatively lower than without CNTs composite electrode (R_{CT}^{-CNTs}= 263.1 ohm). The electrolyte resistance (R_S) purports charge movements through the electrolyte between both electrodes, cathode and anode. (R_S^{+CNTs}= 5.83 ohm, R_S^{-CNTs}= 9.54 ohm)

2) A volume increasing of active material, PVK, happened during charge/discharge process, it caused disjunction between paste and current collector, aluminum foil. In this regard, CNTs seem to act as a binder to attach with current collector relatively and deadened disconnection during the cycling. It is hard to observation of volume changes or thickness changes, but, we observed disjunction of paste and current collector after cycling. Moreover, the condition of composite electrodes was clearer than none CNTs electrode even though it needs more dispersion time to clear form of electrodes (general RPM= ~1500, more strength rate= ~2200 RPM).

The charge/discharge profile shapes are resembled, but the capacities are dissimilar (capacity of –CNTs (Q_{dch}^{-CNTs}) = 87.44 mAh g^{-1} and +CNTs (Q_{dch}^{+CNTs}) = 96 mAh g^{-1} at 1C-rate). The potential of the cells was 3.3 V (vs. Li/Li^+) and the outstretched leg shape below 3.3 V. We assumed this is CNTs effect in our system **(Figure. 24)**.

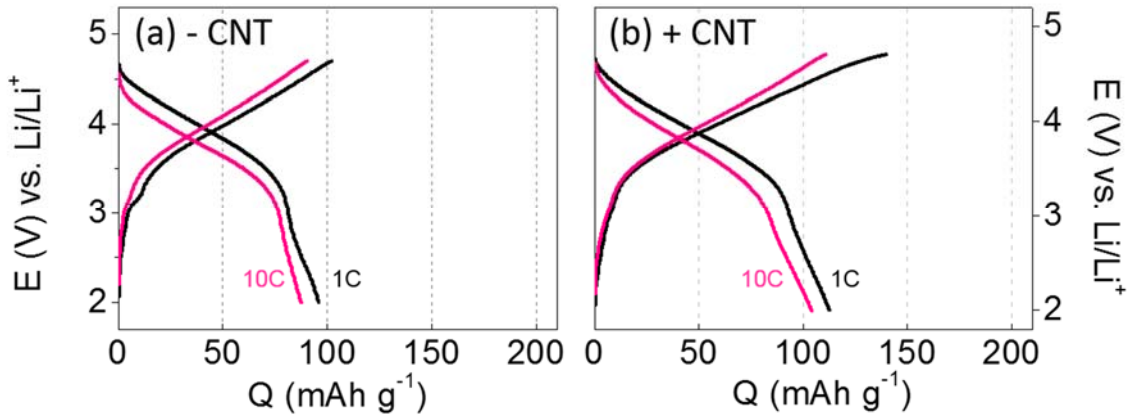

Figure. 24 Charge/discharge profiles of PVK as an active material and PVdF as a binder with or without CNTs. Charge= 1C-rate/ discharge= variable C-rate (1 and 10C).

3.1.2. PVK with PAA-CMC binder in water system

The solvent unconditionally necessary to mix powders (active, binder and conducting agent) in the process of making the electrodes. We using organic solvent NMP to make pastes when using the PVdF binder, while the PAA-CMC binder used with water. That is the difference between two pastes and selection of solvent can soluble binders is important to make ideal electrodes. In this work, we compared with organic solvent or water based electrode in our system which is PVK as an active material. Conclusions so to speak, NMP based PVdF binder was suited for PVK. The evidences of the previous result: (1) the kinetic properties are determined by how fast electron movement on the electrode. Electron movement rate can assumed by CVs during the oxidation/reduction in the electrolyte at several scan rate. The potential gap ($\triangle E_P$) with PVdF is smaller than PAA-CMC at various scan rate ($\triangle E_P^{PVdF}$= 0.25 V, $\triangle E_P^{PAA\text{-}CMC}$= 0.83 V). The small potential gap meaning that the movement of electrons are facilitate, also it can be said to be kinetically fast system **(Figure. 25 (a and b))**. In addition, we can calculated practical capacity with area how much current is flowed without galvanostatically charge and discharge test. The time it takes for oxidation using a scan rate (example. 10 mV/s) calculated and divide the mass of active material (Q_{ch}^{PVdF}= 106.67 mAh g^{-1}, $Q_{ch}^{PAA\text{-}CMC}$= 77.78 mAh g^{-1}) **(Figure. 25 (c and d))**.

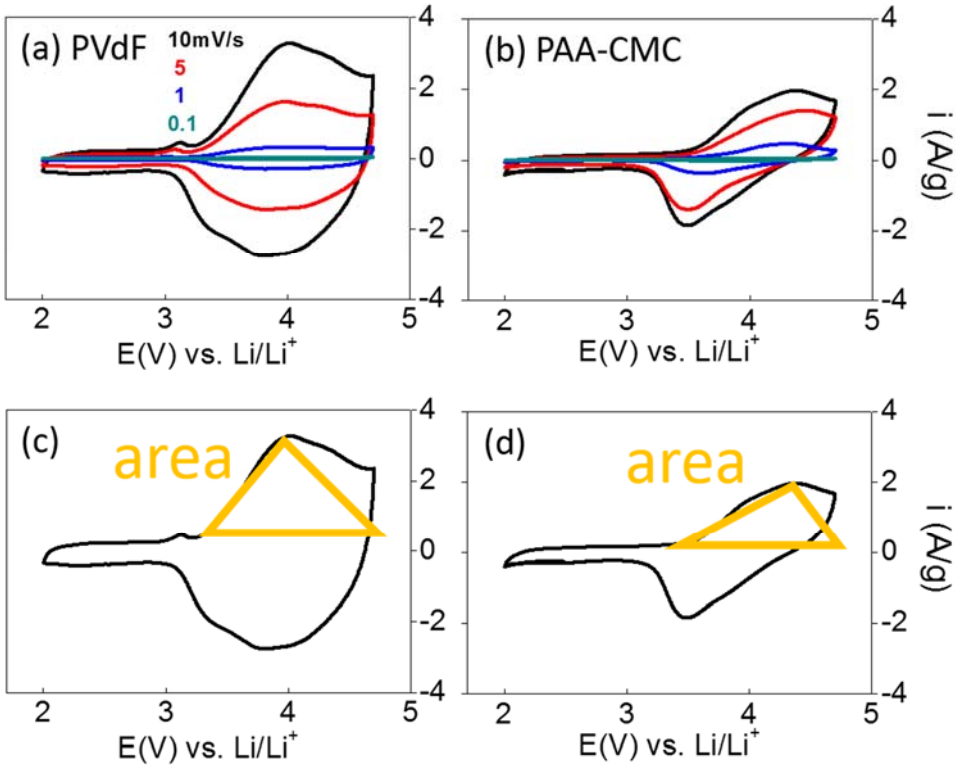

Figure. 25. (a, b) The cyclic voltammograms of PVdF and PAA-CMC binder electrodes with se. Scan rate= 10 mV/s. **(c, d)** How to calculate capacity with cyclic voltammograms with scan rate (10 mV/s).

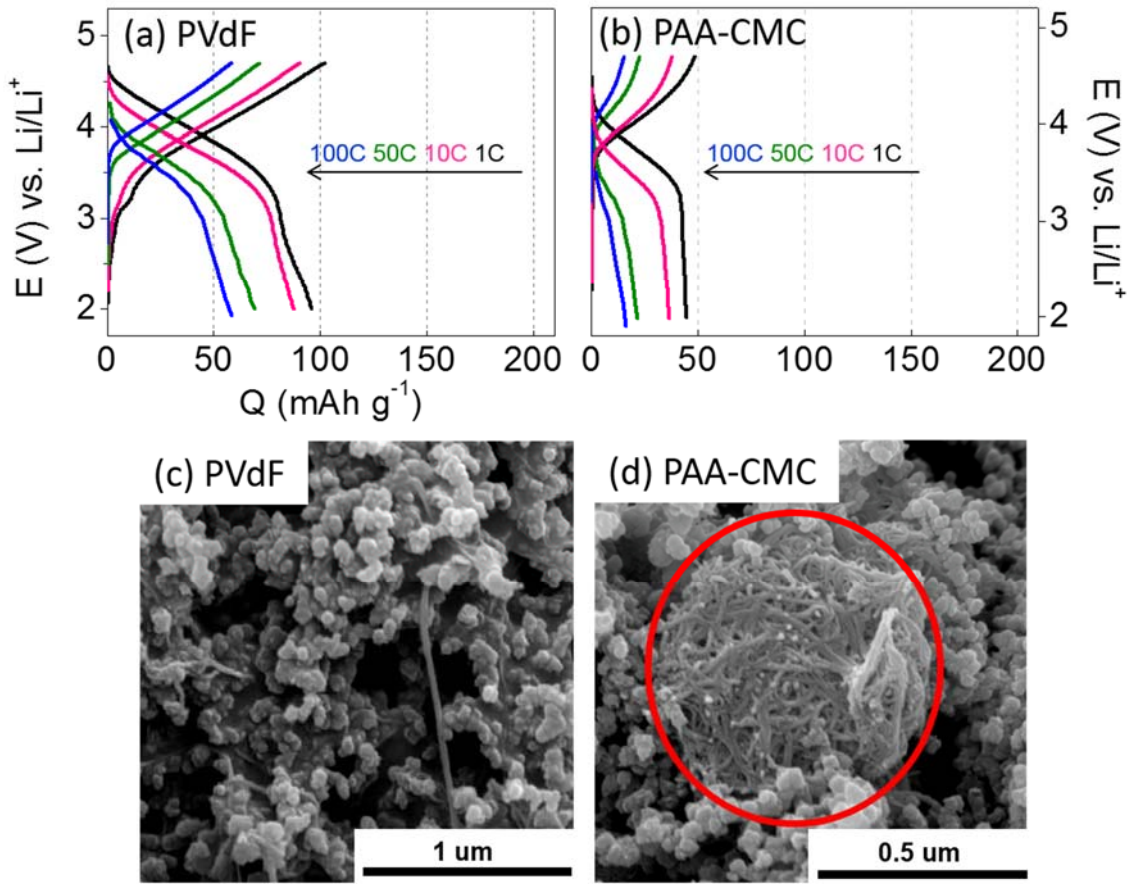

Figure. 26. (a, b) Charge/discharge profiles of composite electrodes with **(a)** PVdF and **(b)** PAA-CMC binder (charge= 1C/discharge=variable). **(c, d)** Scanning electron microscopies of electrode with PVdF of PAA-CMC binder. (The cells were not add CNTs as a secondary conducting agent)

The working potential of the cells is from 2.0 V to 4.7 V versus Li/Li^+ and it can charged at 1C-rate. General half-cell test for lithium ion battery is hard to sufficiently charge with 1C-rate, nonetheless our cells can charged 1C-rate. That is one of evidence to explain the profits of polymer as an active material greatly fast electron transfer in the battery system regardless electrode compositions. **(Figure. 26. (a, b))**

Relatively low capacity is due to partial aggregations on the current collector and it confirmed by SEM images for obvious chunks. Partial aggregated grains were showed which did not dispersed in water, PVK. That grains acted as dead volume and could not express their capacity. (**Figure. 26 (c and d))**

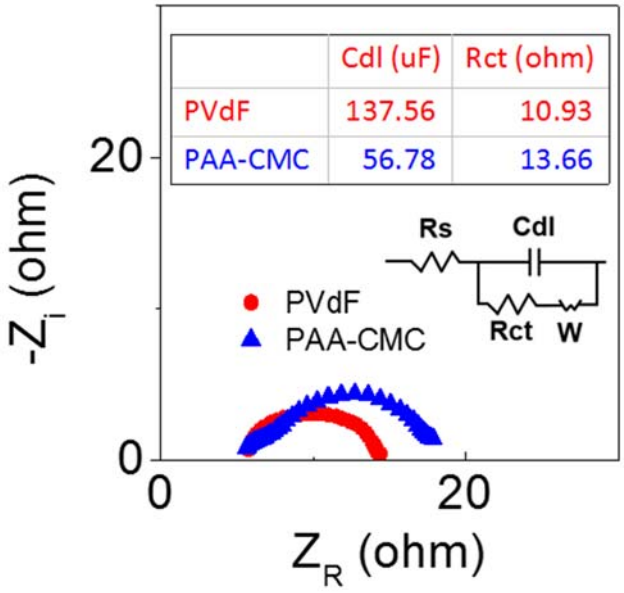

Figure. 27. Impedance spectra with binders at peak potentials 4.2 V (vs. Li/Li^+) from 200 kHz to 0.1 Hz.

Coin-type half cells were tested to investigate impedance characteristics and calculate fitting values with equivalent circuit. The charge transfer resistance (R_{CT}) is similar, but, dead volume produced low capacitance in terms of low active area comparatively. These dead volume caused the low kinetics, capacity (mAh g^{-1}) and capacitance (F=C/V, coulomb/volt) (**Figure. 27**).

Summarized the contents of up to now, CNTs as secondary conducting agent helped binding with current collector or all components. The secondary conducting agent, also, improved movement of charges from active sites to current collector. PVK was confirmed that it dispersed well in the organic solvent, NMP, than in the aqueous solution. Dead volume was identified because of aggregation or bindles in the aqueous solution partially by SEM image. Dispersed PVK in NMP caused fast charge and discharge system due to the facile electron transfer, low resistance and high capacitance (**Figure. 28**).

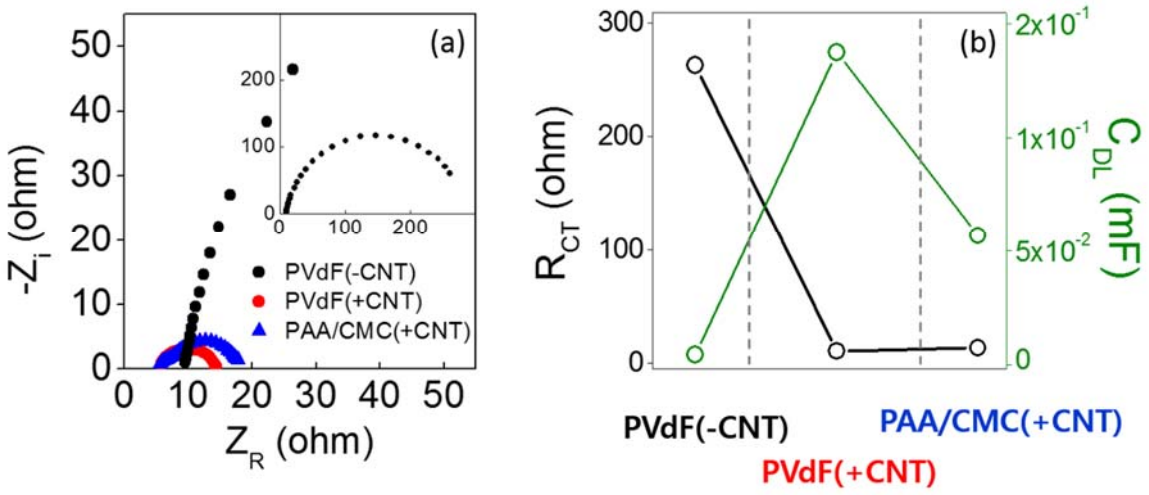

Figure. 28. Effects of CNTs as a secondary conducting agent and PVdF as a binder. (a) EIS, (b) calculated values of resistance and capacitance.

3.2. Conductive binder PEDOT for composite electrode

An 1D organic redox-active material is composited with another 1D conductive material for rechargeable batteries. PVK and PEDOT:PSS are used as the redox-active and conductive 1D materials, respectively. Due to their extreme anisotropic geometry, the two polymers are expected to be inter-tangled with each other, showing an kinetically ideal model system in which each redox-active moiety of PVK is supposed to be directly connected with the conducting pathways of PEDOT:PSS. In addition to the role of conductive agents providing kinetic benefits, PEDOT:PSS works as an efficient binder that guarantees enhanced electrochemical performances with only a tenth of the amount of a conventional binder (polyvinylidene fluoride or PVdF). The benefit of gravimetric energy density gain obtained with the conductive binder comes mainly from efficient spatial coverage of binding volume due to the low density of PEDOT:PSS (**Figure. 29**).

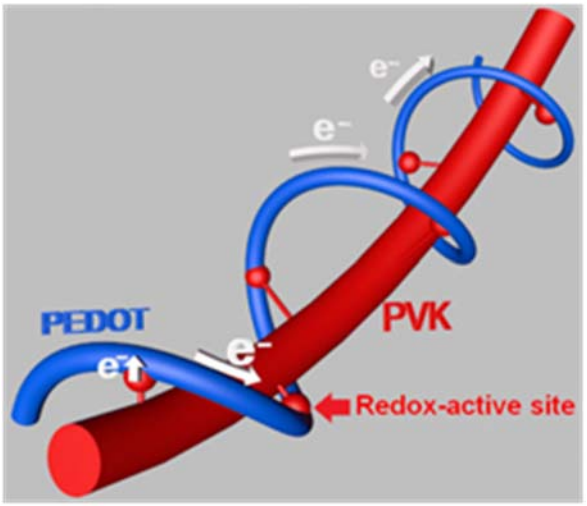

Figure. 29. Schematic picture of a tangle of PVK (red) and PEDOT:PSS (blue). Electrons are transferred from electroactive sites (red balls) of PVK to PEDOT:PSS and then moves along PEDOT:PSS strand in a fast way.

As a schematic model system guaranteeing fast electron transfer, we could imagine that each active site of redox-active polymer (red ball in **Figure 29**) is directly connected to polymeric backbone of conducting polymer (blue line).

3.2.1. PVK / PEDOT:PSS composite electrodes

The model system to motivate this work (**Figure. 29**) was materialized with PVK as an redox-active polymer and PEDOT:PSS as an conducting polymer. PVK is a polyethylene backbone with redox-active carbazole moieties. PEDOT:PSS is a composite of two different polymers that are interacted electrostatically. Homogeneous and well mixed composites were achieved without any indication of agglomerations of respective polymers. At least in terms of physical configuration, the model system we intended to build is believed not to be objected.

Binders are used to keep mechanical integrity of electrode composites on current collectors. They provide cohesion between components of composite electrodes as well as adhesion onto current collectors. Conventional binders such as PVdF are not significantly meaningful from the viewpoint of electric and ionic pathways. On the other hand, PEDOT:PSS used in this work plays two-fold roles as a conductive binder (not only as a conducting agent but also as a binder). Therefore, expected is significant reduction of charge transfer resistance between redox-active sites of PVK and electric pathways consisting of carbon black (**Figure. 30**).

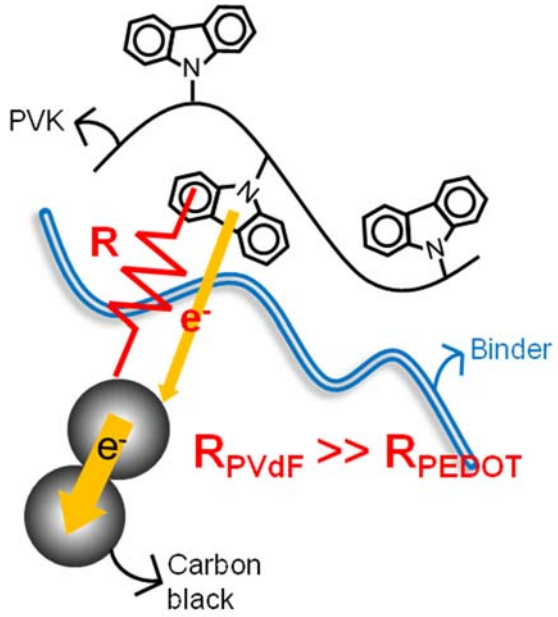

Figure. 30. Benefits of a conductive binder (PEDOT:PSS) compared with a conventional binder (PVdF). Charge transfer resistances (R) are reduced with PEDOT:PSS.

Binding force of PEDOT:PSS was considered to be strong enough to obtain successful coating just with 1 wt. % PEDOT:PSS (**Figure. 31 (c)**). With the same amount of binder (1 wt. %), however, the conventional binder PVdF did not result in conformal coating on aluminium current collector (**Figure. 31 (b)**). At least with 10 wt. % PVdF, good quality of composite coating was realized (**Figure. 31 (a)**). It must be a benefit to obtain good composite coating on current collector with smaller amount of binder. The gain of relative contents of redox-active mass leads to higher gravimetric capacity resulting in higher energy density.

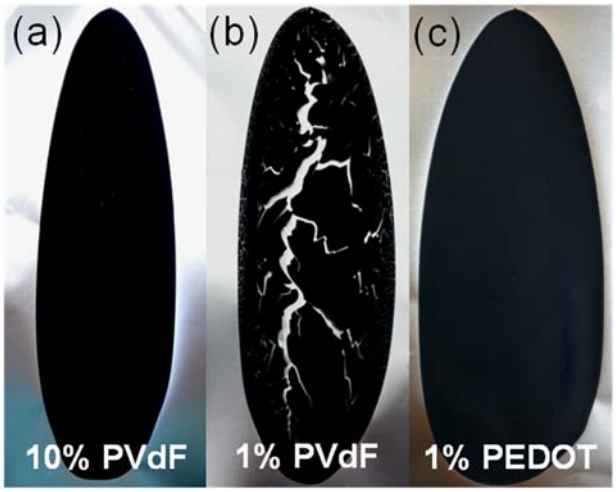

Figure. 31. Coating quality of composites based on PVdF and PEDOT binders. Aluminium foils were used as substrates. Poor adhesion was observed with 1 wt. % PVdF (b) while the composite was successfully coated with the same amount of PEDOT:PSS (c).

Spatial coverage of binders within electrode composites partly explains why such a small weight of PEDOT:PSS is enough to bind other components. On morphological investigations by SEM, particles (presumably, agglomerates of carbon black) are clearly identified in the PVdF-containing composites (10 wt. % in **Figure. 32 (a)**). With PEDOT:PSS, however, the whole body of a composite looks monolithic like some particles embedded in a wax-like matrix (**Figure. 32 (b to d)**). Even 1 wt. % PEDOT:PSS provided enough volume which other components stick to. Most of featured morphology was swallowed by the matrix with more than 5 wt. % PEDOT:PSS. That is to say, lower density of PEDOT:PSS results in efficient binding architectures. Densities of composite electrodes of 10 wt. % binders were estimated at 0.43 g cm^{-3} for PVdF and 0.23 g cm^{-3} for PEDOT:PSS. Composite with 1 wt. % PEDOT:PSS still showed density lower than that of PVdF composite (0.27 g cm^{-3}) even if content of the low density binder was reduced. As a rule of thumb, higher density is preferred for redox-active

materials (PVK in this work) to achieve high energy density. On the other hand, lower density would be a good choice for binders because the same mass can provide more binding volume in a composite space.

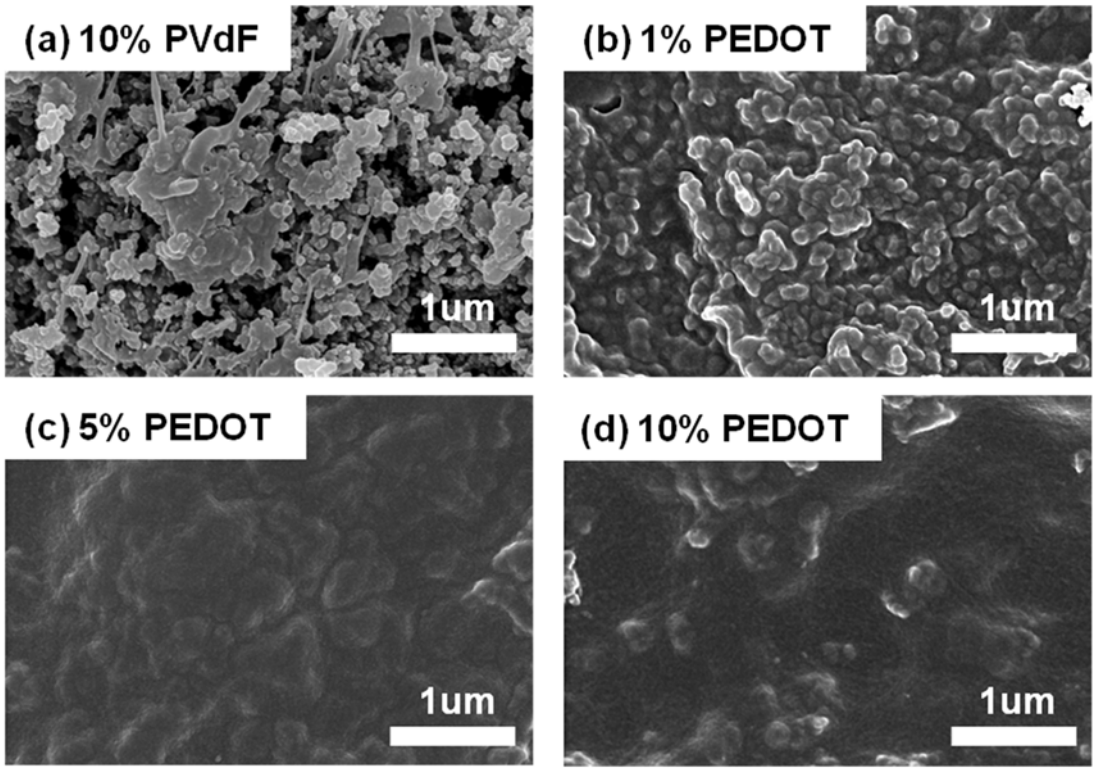

Figure. 32. Morphological SEM images of composite electrodes. Composites based on various PEDOT contents were compared with PVdF-containing one.

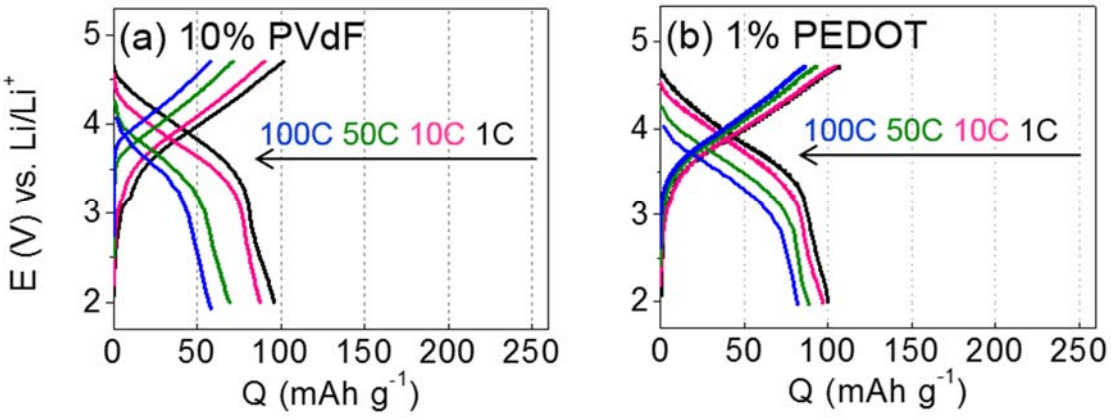

Figure. 33. Charge/discharge profiles of binder dependent performances with PVK and Super P. Charge= 1C-rate/discharge= variable.

PEDOT:PSS-containing composite electrodes showed kinetically enhanced faradaic electrochemistry, compared with its PVdF-containing counterpart. It should be emphasized that PEDOT:PSS was used a tenth as much as that of PVdF. At low discharge rates less than 1C, the two composite materials delivered similar capacity (**Figure. 33 (a, b)**). At higher discharge rates, however, PEDOT:PSS prevailed over PVdF in terms of capacity ($Q_{binder}^{C\text{-}rate}$) : Q_{PEDOT}^{100C} = 79.5 mAh g^{-1} (80 % of Q_{PEDOT}^{1C}) while Q_{PVdF}^{100C} = 56.7 mAh g^{-1} (59 % of Q_{PVdF}^{1C}).

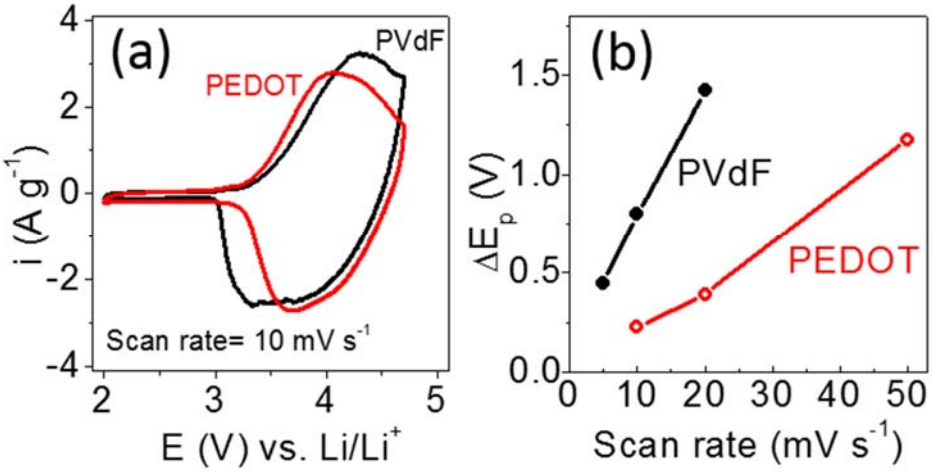

Figure. 34. (a) Cyclic voltammograms (CVs) scanned at 10 mV s^{-1}. (b) Scan rate dependency of peak-to-peak potential gap ($\triangle E_p$).

Peak-to-peak gap ($\triangle E_p$) obtained from cyclic voltammograms (CVs). Increasing of scan rate, the values gap of PEDOT delta is relatively small, it can be seen that the kinetics of PEDOT is fast. (**Figure. 34 (b)**) In addition, the potential gap during the oxidation and reduction of the composite electrode is small comparatively even though the current amount is small (**Figure. 34 (a)**).

Charge transfer resistance (R_{CT}) measured from impedance spectra also supported the superior kinetics of PEDOT:PSS-containing composites (**Figure. 35**).

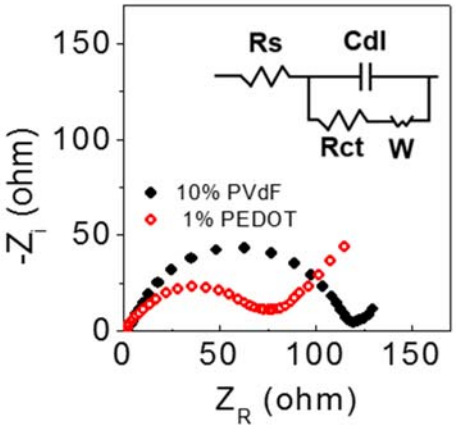

Figure. 35. Electrochemical impedance spectra at peak potentials (4 V for PEDOT and 4.2 V for PVdF) from 200 kHz to 0.1 Hz.

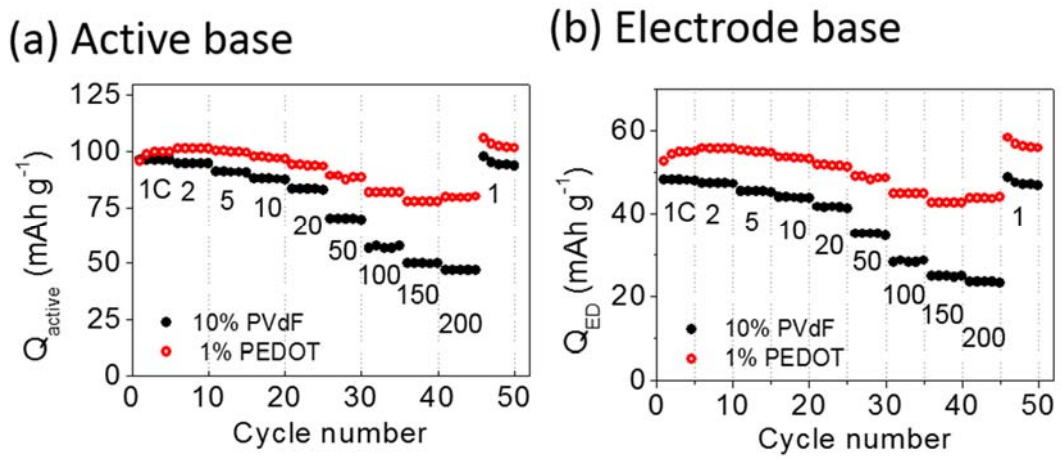

Figure. 36. Capacity depending on discharge rates at a fixed charge rate (1C). Capacity was normalized by mass of PVK (a) or composites including all components such as PVK, binder and carbon black (b).

As shown in potential profiles, higher capacities per mass of PVK were obtained with PEDOT:PSS especially at high rates (**Figure. 36 (a)**). The capacity difference between the binders becomes more contrasted when the whole mass of electrode is used as the basis to normalize capacity (**Figure. 36 (b)**). Therefore, it can be said that higher energy density as well as power density is realized by the use of PEDOT:PSS.

3.2.2. PEDOT:PSS contents modification

PEDOT:PSS contents in composite electrodes were varied. If the conductive binder were guessed to be helpful, the comparison counterpart would be the conventional non-conductive binder, PVdF. We should consider, however, that the conductivity of PEDOT:PSS is still lower than that of carbon black. Binders, whether they are conductive or not, would not be required only if the physical integrity of electrode composites is guaranteed. That is to say, the minimized binder content that barely manages to bind electrode components would be the optimized value. The discussion consisted with measured conductivities of composite electrodes based on PVdF or PEDOT:PSS (**Figure. 37**).

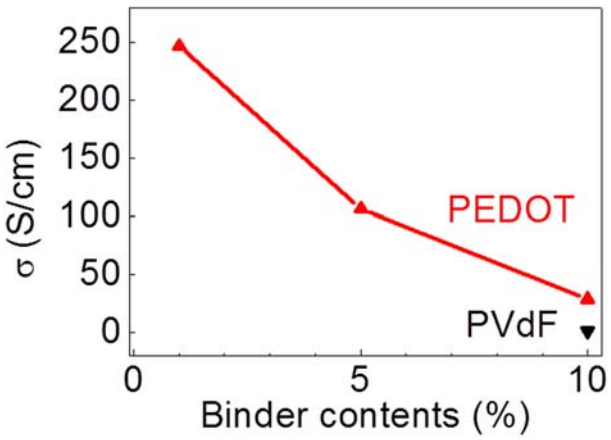

Figure. 37. Electric conductivities (σ) of PEDOT:PSS of various contents versus 10 wt. % of PVdF.

At the same composition (10 wt. %), PEDOT:PSS-containing composites was 30 times as conductive as its PVdF-containing counterpart: 30 S cm^{-1} for PEDOT:PSS versus 1.2 S cm^{-1} for PVdF. As binder contents decreased to 1 wt. %, conductivity of PEDOT:PSS-containing composite was impressively enhanced to 250 S cm^{-1}. PEDOT:PSS should be considered not as a main conduction pathway (which carbon black is responsible for). Therefore, higher contents of PEDOT:PSS led to slower kinetics of carbazole electrochemistry, showing wider $\triangle E_p$ in CVs (**Figure. 38 (a)**) and higher charge transfer resistance (R_{CT}) in impedance spectra (**Figure. 38 (b)**). R_{CT} was obtained by nonlinear least square fitting with a model. The equivalent circuit model (the inset of **Figure. 38 (b)**) represents the

electrochemical process of this work roughly by a single R_{CT} with capacitance for double layer formation (C_{dl}) and Warburg element (W) for diffusion of lithium ions. The depressed semi-circles indicate that non-ideal single charge transfer process is involved or that multiple (probably two) charge transfer processes are highly overlapped due to the similar values of time constants. R_{CT}, estimated by diameter of semi-circles, increased with PEDOT contents, indicating slowing charge transfer kinetics: 66, 74 and 180 ohm for 1, 5 and 10 % PEDOT, respectively. In addition, 1 wt. % PEDOT:PSS was superior to 5 and 10 % counterparts in terms of rate capability (**Figure. 38 (c)**) without any problems in capacity retention during cycling at least up to the 100th cycle (**Figure. 38 (d)**).

The 1% PEDOT has the smallest resistance than other conditions, even it showed lower capacitance than 10 % PVdF. Less resistances, R_S and R_{CT}, in the cell signified the movement of the electron that can move rapidly (**Table. 2**).

Code	R_S	Capacitance (uF)	R_{CT}
10 % PVdF	4.20	8.32	111.3
1 % PEDOT	0.94	6.45	65.58
5 % PEDOT	2.142	2.61	73.88
10 % PEDOT	6.00	5.27	175.80

Table. 2. Values of variable cells by electrochemical impedance spectra at peak potential (4 V for PEDOT and 4.2 V for PVdF) from 200 kHz to 0.1 Hz. All values were calculated Zview.

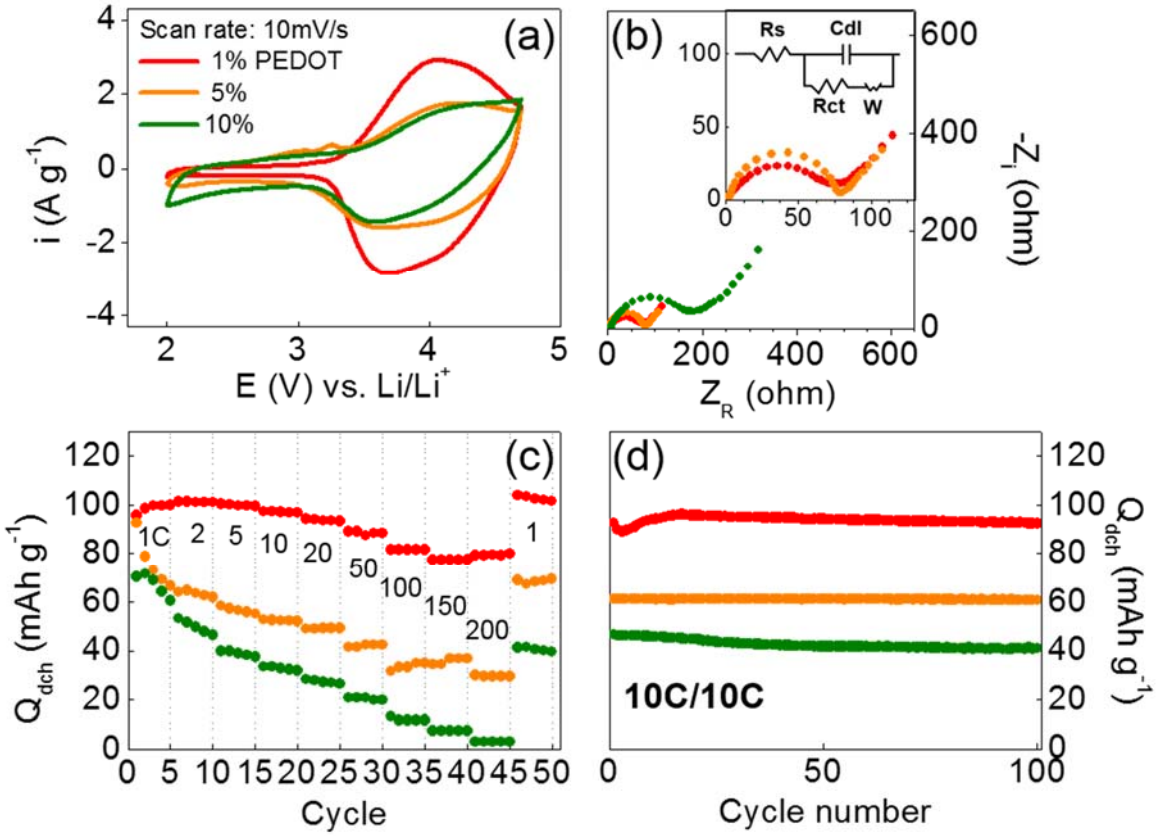

Figure. 38. PEDOT contents dependency of electrochemical performances. (a) CVs. (b) Electrochemical impedance spectra. (c) Capacity depending on discharge rates at a fixed charge rate (1C). (d) Capacity retention with cycles at 10C/10C (charge/discharge).

3.2.3. Conductive potential window of PEDOT:PSS

PEDOT:PSS is conductive only in its oxidized state. It turns into an insulator at potential negative enough to reduce the polymer. In aqueous electrolytes, reduction and oxidation peaks are clearly observed between -0.2 V and -0.5 V versus Ag/AgCl (equivalent to +2.8 V to +2.5 V versus Li/Li^+).[71] If the value were correct in the electrolyte used in this work, the reduction potential of PEDOT:PSS would be located within our potential window of operation (4.5 V to 2.0 V versus Li/Li^+). There is every possibility that PEDOT:PSS could work as an insulating material to hinder electron transfer or conduction during discharge before the cells reach the cut-off potential at 2.0 V. Therefore, we checked the reduction potential of PEDOT:PSS in the organic electrolyte used in our cells. Three different pairs of redox peaks were observed as indicated by Greek letters in **Figure. 39 (a)**. Even if we are not sure of which electrochemistry is responsible for each peak, it is clear that PEDOT:PSS is conductive in the operational potential range of our PVK cells. There were no significant changes of impedance spectra from 4.0 V up to 1.0 V. Therefore, PEDOT:PSS in cells can work as a conductor to support kinetics of composite electrodes.

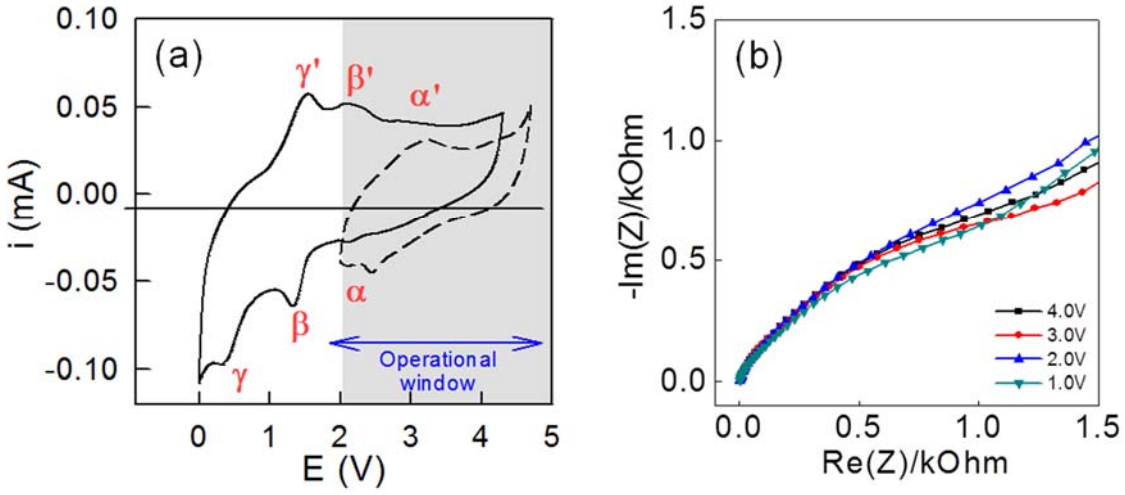

Figure. 39. Conductive potential window of PEDOT:PSS. (a) CV is obtained at 10 mV s^{-1}. Three pairs of peaks related to faradaic reactions are observed. (b) Electrochemical impedance spectra at various potential.

3.2.4. PVK/PEDOT:PSS composites with polymer gel electrolyte

As a pre-step of building all-polymer rechargeable batteries, a polymer gel electrolyte[75] was applied to our PVK/PEDOT:PSS composite systems. The almost-all-polymer cells consists of polymers including PVK as an active material, PEDOT:PSS as a binder, PVA-CN as a polymeric gel skeleton and a polyolefin separator. Non-polymer part includes carbon black and liquid electrolyte, both of which are embedded in polymer matrices.

PVA-CN solubilized in electrolyte at room temperature was introduced into cells as a liquid phase. After the electrolyte containing PVA-CN was fully impregnated into porous composite electrodes, gelation was initiated at 60 ^{o}C. Low density of PEDOT:PSS-based composites (rather than PVdF-based one) is helpful in terms of wetting. The resultant cells have continuously interconnected polymer network though whole volume of cells.

Up to 50C, introduction of gel electrolyte into PEDOT:PSS-containing PVK cells slowed the kinetics of carbazole electrochemistry down due to its ionic conductivity a little bit lower than that of liquid (**Figure. 40**). Therefore, gel electrolyte delivered lower capacities at the same discharge rates than liquid electrolyte in the cells with the same binder, PEDOT:PSS. However, the gel-based cells with PEDOT:PSS was still superior to the liquid-based cells with PVdF in terms of rate capability. Beyond 50C, more interestingly, capacity decay of PEDOT:PSS-containing cell with increasing C rate was significantly depressed with the gel electrolyte. At 100C to 200C, the capacities of gel electrolyte were comparable to those of liquid one. We reported that the PVA-CN gel electrolytes can provide higher capacities at fast discharge rates due to its high transference number of lithium ion.[75] Concentration polarization experienced at fast discharge situations can be overcome with the gel electrolyte. The inter-tangled network of RP and CP utilized the benefit of gel electrolyte efficiently, which might be caused by a good mixing between polymeric strands. On the contrary, the benefit of gel electrolyte at high rates was not observed with PVdF.

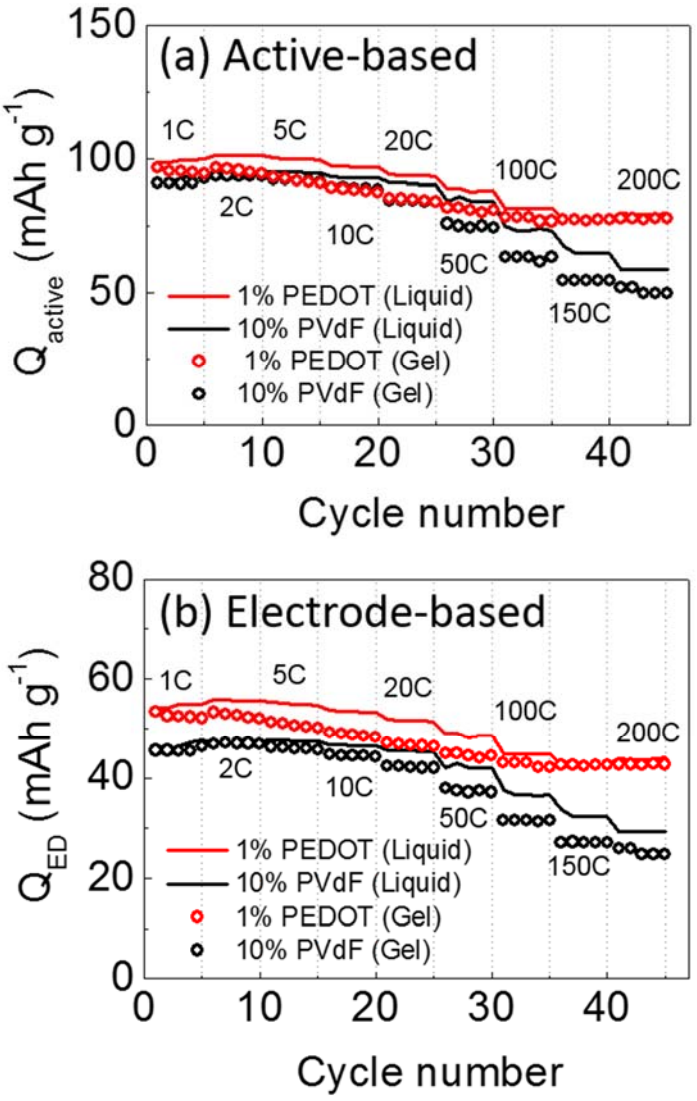

Figure. 40. Electrochemical performances of quasi-all-polymer cells of PVK, PEDOT:PSS, PVA-CN and polyolefin. Capacities depending on discharge rates at a fixed charge rate (1C) were normalized by mass of PVK (a) or composites including all components such as PVK, binder and carbon black (b).

IV. CONCLUSION

In our work, we tried to proof organic materials, especially polymers, as an active material for rechargeable batteries. The organic active materials were superior to fast electron transfer during the repeated oxidation and reduction. Nevertheless small molecular weight materials had dissolve problem in the electrolyte. Polymerization of the materials with low molecular weight was one of solution to solve the problem. Because of that, we tried to realize a kinetically facile model system in which a 1D polymer tethered with redox-active sites is tangled with another 1D polymer providing electric pathways. Each redox-active molecule is supposed to be directly connected with the conducting pathways. PVK and PEDOT:PSS were used as the redox-active and electrically conducting 1D materials, respectively. PEDOT:PSS worked as a binder as well as a conductive agents. Electron transfer kinetics of PVK was significantly enhanced by 1 wt. % PEDOT:PSS even if only a tenth of the amount of a conventional binder (PVdF) was used. The benefit of gravimetric energy density gain obtained with the conductive binder comes mainly from efficient spatial coverage of binding volume due to the low density of PEDOT:PSS. Quasi-all-polymer batteries was realized with PVK as an active material, PEDOT:PSS as a conductive binder and PVA-CN as a gel frame. We believe that polymeric active materials have high possibility as an alternative to conventional inorganic electrode materials such as $LiCoO_2$ and $LiMn_2O_4$ at least in niche markets in which high flexibility and high power demands are required. For practical applications, however, additional endeavour should be devoted. For example, energy density of composite electrodes should be enhanced by decreasing the content of conducting agent such as carbon black into less than 10 wt. %.

VI. APPENDIX

6.1. Procedure of make coin-type half cells

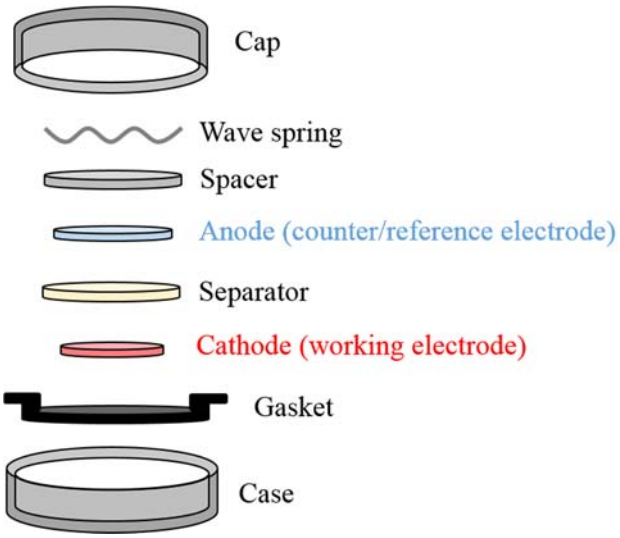

Figure. A. 1. Mimetic diagram of coin-cell.[76]

① Set the gasket in the case (prevent of air and electrolyte leakage).

② Place a cathode in it (Width of composite electrode; **14Ø**).

③ Place a separator between cathode and anode; **18 Ø**.

④ Add an appropriate amount of electrolyte.

⑤ Place an anode (Lithium metal as a counter and reference electrode); **16 Ø**.

⑥ Place the spacer (fill the empty space).

⑦ Place the wave spring.

⑧ Close the cell with the cap.

6.2. Poly (anthraquinonyl sulfide), (PAQS)[33]

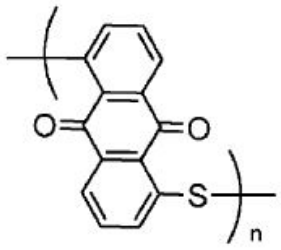

Scheme. A. 1. The structure of PAQS.

One of the problems of the organic compounds was soluble in electrolyte and polymerized organic compounds to solve dissolve in electrolyte. Ring-sulfur bond acting as orthotic to prevent dissolved in the electrolyte. Poly (anthraquinonyl sulfide) (PAQS) was studied which is a type of carbonyl active material (**Scheme. A. 1)**. The sample was synthesized simple poly-condensation, Phillips method (**Scheme. A. 2**) by Yang research group.[77]

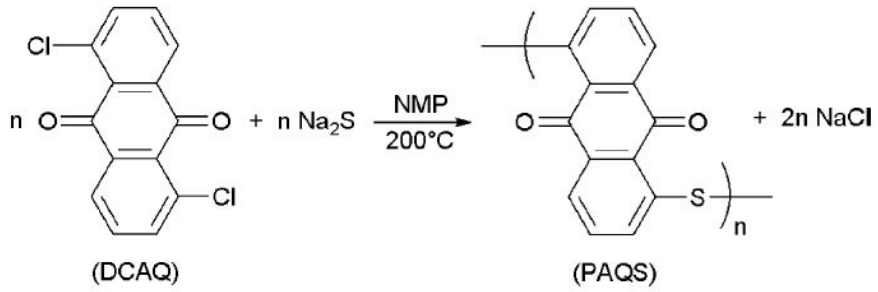

Scheme. A. 2. The schematic of synthesized process of PAQS with Phillips method.

Figure. A. 2 showed FR-IR of the PAQS. The absorptions at 1130 cm^{-1} and 1415 cm^{-1} bands in the PAQS spectrum which designated ring-sulfur and di-substituted ring to stretching of the sulfur, individually. The absorption at 1570 cm^{-1} indicated aromatic C=C.

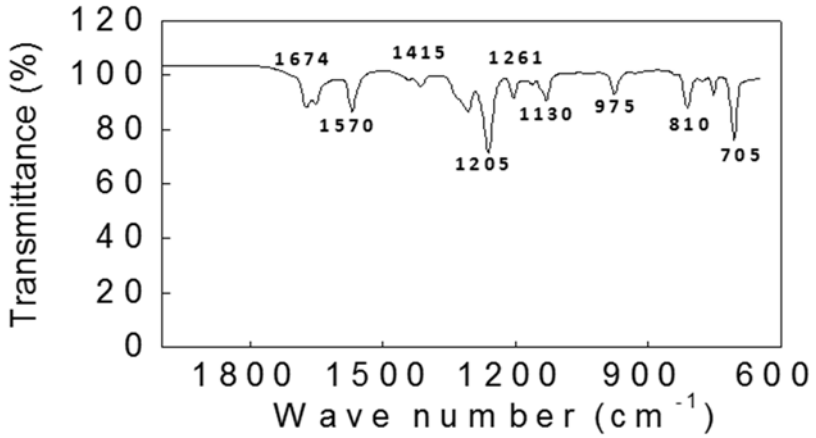

Figure. A. 2. FT-IR of synthesized PAQS powder. Range of wave number= 2000~650 cm^{-1}.

The formation of synthesized PAQS was verified by elemental analysis. The measured value of Carbon, Hydrogen and Sulfur in PAQS is 68.74 %, 2.87 % and 10.25 %, respectively. The calculated value of C, H and S in PAQS is 70.59 %, 2.52 % and 13.45 %. It measured by *Thermo Scientific*, Netherlands, *Flash 2000*.

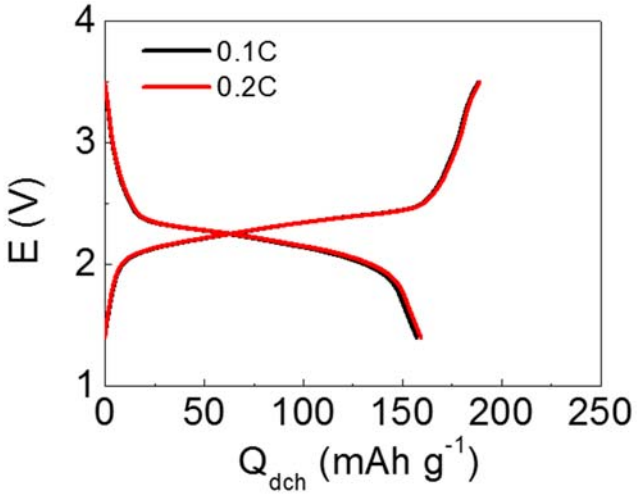

Figure. A. 3. The profiles of PAQS at 0.1C during the charging.

The constant current charge/discharge test was examined with half-type coin cell. The configuration of the working electrode was PAQS: PVdF: conducting agent, Super P (4: 2: 4, wt. %). 1M $LiClO_4$ in 1, 3-dioxolane (DOL)/ dimethoxyethane (DME) (2/1 wt. %) used as an electrolyte. First cycle capacity and columbic efficiency were similar with second cycle, 220/ 219 mAh g^{-1} and 99/ 96 %. Practical capacity resembled theoretical capacity of the PAQS, 225 mAh g^{-1} (**Figure. A. 3**).

6.3. Denpol containing anthraquinone terminated dondrons (AQ-*ter*-denpol)

Dendronized polymers (denpols) are uniquely hyperbranched macromolecules carrying dendritic wedges (dendrons) densely attached along a linear polymer backbone.[78] Owing to the high degree of control that can be exerted over their size and shape as well as the ability to place a wide variety of chemical functionalities at spatially defined locations,[79-80] the denpols are excellent candidates for a variety of materials applications such as biomaterials,[81] drug delivery and optoelectronics.[82] Thereby, the preparation of novel well-defined denpols with the dendrons containing building blocks designed for specific purposes (*i.e.*, nature/shape/functionality/size) remains not only a topical challenge but also these materials can represent a key stage in the ongoing evolution of macromolecular and supramolecular chemistry.[79, 82-83]

Stimulated by the fast-growing demand for the construction of sustainable, low-cost, and functional energy storage systems, we have now become sought to establish the utility of redox-active denpols for organic rechargeable batteries. It is believed that the usefulness of these denpols derives mainly from their multivalent and highly functionalizable structures that enable the crowded redox-acitve functional groups, and from their unique backbone conformations that may result in interesting morphological dynamics and kinetics. In line with these aspects, we report herein the first synthesis of a denpol containing multi-anthraquinone (AQ)-terminated dendrons (**AQ-*ter*-denpol**) by means of living ring-opening metathesis polymerization (ROMP)[84] using the third generation Grubbs catalyst ($(H_2IMes)(pyr)_2(Cl)_2Ru$=CHPh (**G3**)) Grubbs catalysts. Besides, evaluation of **AQ-*ter*-denpol** as a cathode for rechargeable Li-ion batteries is, in preliminary form, investigated.

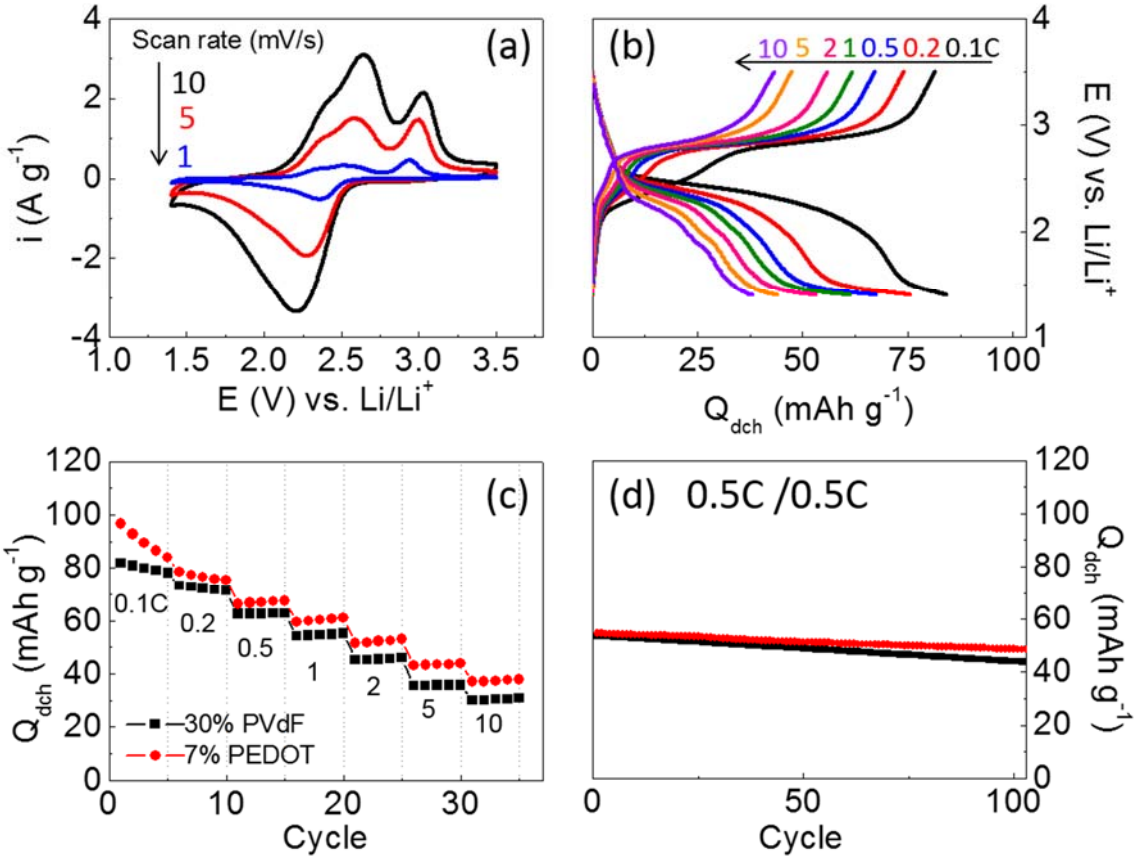

Figure. A. Z1. (a and b) Cyclic voltammograms (a) and potential profiles during galvanostatic discharging (b) of AQ-*ter*-denpol with PEDOT as a binder in a coin half cell. (c and d) Rate capability (c) and cyclability (d) of AQ-*ter*-denpol with PEDOT or PVdF as a binder in a coin half cell.

Figure A. Z1 (a) and **(b)** show cyclic voltammograms of AQ-*ter*-denpol and its potential profiles during galvanostatic discharges, respectively. The cells containing AQ-*ter*-denpol were charged at 0.1 C before discharging. 1C was defined as 140 mA g^{-1}, which is the current to extract a whole energy for 1 h. To investigate the redox activity of AQ-*ter*-denpol, coin-type cells (**Figure. A. Z1**)[10] were electrochemically tested with 1 M $LiPF_6$ in ethylene carbonate (EC)/dimethyl carbonate (DMC) (5:5, v/v) as an electrolyte. A mixture of AQ-*ter*-denpol and carbon black with PVdF (polyvinylidene fluoride) or PEDOT (Poly(3,4-ethylenedioxythiophene)) as a binder (2:5:3 or 0.5, wt. ratio) deposited on aluminum foil was used as a working electrode while lithium metal was used as a counter electrode. AQ-*ter*-denpol was not soluble in carbonate solvents, guaranteeing stable performances without losing immobilized mass by dissolution. Insolubility attributed to the stiffening of the polymer backbone by the dendritic substituents[85] is the advantage of AQ-*ter*-denpol when considering other anthraquinone-based polymers such as a poly(anthraquinonyl sulfide) (PAQS) and poly(vinylanthraquinone)

(PVAQ)[86-88] are difficult to use in carbonate solvents due to their solubility.

Two different anodic processes at 2.52 V and 2.93 V assigning to one and the other carbonyl groups of anthraquinones were reversibly paired with a single cathodic process at 2.37 V (read from 0.1 mV s^{-1} in **Figure. Z (a)**), confirming that AQ-*ter*-denpol is redox-active and operable as an active material in the polymer Li metal batteries. The potential difference of AQ-*ter*-denpol between the cathodic peak and the anodic peak at the more negative potential (ΔE_{p1} = 0.15 V) was estimated smaller than that of PVAQ (0.19 V) and comparable to that of PAQS (0.33 V), providing the possibility of faster kinetics. The reversible capacity based on the redox activity of AQ-*ter*-denpol was estimated at 84 mAh g^{-1} at 0.1 C (**Figure. Z (b)**). Its rate capability was enhanced (**Figure. Z (c)**), considering ~50 % of capacity at 0.1C was achieved at 10C, the current rate one hundred times as high as 0.1C (cf. less than 28 % for PAQS at 10C[34]). Also, its stability was guaranteed during cycling charge and discharge processes (**Figure. Z (d)**). Morphological characteristics of the polymeric films of AQ-*ter*-denpol supports the improved kinetics (**Figure. Z (e** and **f)**). Dendritic extension of the polymer provides more available contact with electric pathways by carbon blacks as well as ionic pathways by electrolyte, keeping the continuity of its own structure to enable electron hopping from an active site to another.

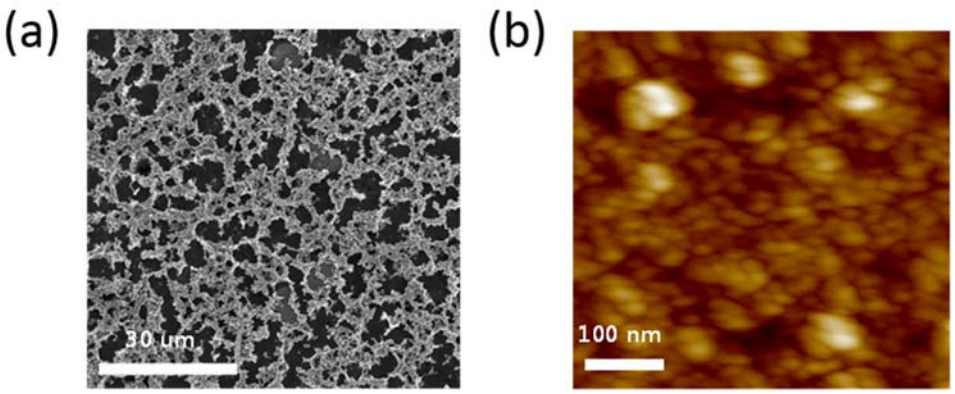

Figure. A. Z2. (e and f) SEM (e) and AFM (f) images of polymeric films of AQ-*ter*-denpol.

VII. ACKNOWLEDGEMENTS

우선, 끊임없이 지원해주신 송현곤 교수님께 감사의 말씀을 전합니다. 언제나 학생의 미래를 위한 너그러운 이해심과 조언을 아끼지 않는 교수님께서 계셨기에 제가 더 많은 용기를 낼 수 있었습니다. 감사합니다!!!

그리고, 우리 eclat 멤버들 감사합니다.

항상 이 곳을 빨리 떠나자며 버릇처럼 얘기하곤 했는데, 아직도…^^ 비록 다른 학위지만 졸업동기인 김영수박사님! 우리 빨리 떠나용~~~ 저 보실 때 마다 무섭다고 피하시던 노현국박사님, 저 무서운 사람 아니니까 도망가지 말아주세요. 입학할 때부터 정신적 지주셨던 이명희 연구원님, 언니~~~ 지금까지 더 많은 시간을 함께하지 못해 아쉽지만! 아직 시간이 있으니 계속 제 정신적 지주가 되어주세요 싸랑해용^^ 언제나 옆자리에서 아낌없는 조언으로 저의 방향을 잡아주셨던 박한샘 미래박사님, 오빠~~~어서 빨리 좋은 소식으로 하하하호호호 웃을 날 만들어 주쎄용. 갑자기 뒤에서 툭치며 “뭐하냐?” 라고 관심 가져주셨던 유부남 고영훈 미래박사님, 콜라 줄이시고 2세 기대할게요 으흐흐흐. 항상 먹는 얘기로 혼연일체가 되었고 ‘음식을 남기는 것은 음식에 대한 예의가 아니다’ 라는 명언을 남겨주신 김태희 미래박사님, 우리 밖에서 만났더라면 더 친하게 지낼 수 있었을 텐데… 여튼 빨리 국수 먹게 해주세요! 제일 비슷한 시기에 학교에 와서 같이 적응해나갔던 착한 척 하는 조윤교님, 미래박사라고 하기엔 아직 많이 남았어… 졸업하는 그 날이 오긴 할까? 이젠 제발 잘생겨지자^^ 맨날 정신 사납다고 뭐라 해도 웃고 넘어가주는 황치현님, 아직 까마득하긴 하지만 돈 많이 벌어서 맛있는 거 많이 사준다고 한 거 잊으면 안되 치현오빠! 성질 고약한 나 만나서 애먹었을 우리 강민선, 나도 제대로 못하면서 맨날 뭐라 하기만해서 미안했어 민선아~~~ 그런데 앞으로도 계속 그럴 거야^^ 같이 운동하러 가자! 얼굴만 봐도 성질 나게 하는 특별한 재주를 가진 이동규, 너의 핸드폰번호를 지울 날이 가까워지고 있으니 기대해^^ 미국에서 열심히 공부하고 즐기고 있을 김은희, 건강하게만 지내길… 우리 다시 만날 날이 오겠지? 잠깐이지만 좋은 기억만 남아 있는 윤다은, 너 너무 귀여운 것 같아. 시크하지만 귀여운 전유주, 앞길이 멀다 유주야… 항상 생기 넘치고 건강한 너니까 뭐든지 잘 할 수 있을 거라고 믿어, 화이띵!

긍정덩어리, 에너지의 원천 박기수 대리님 앞으로도 긍정의 힘 부탁 드려용.

V. REFERENCES

1. Armand, M.; Tarascon, J. M., Building better batteries. *Nature* **2008,** 451, 652-657.

2. Palacin, M. R., Recent advances in rechargeable battery materials: a chemist's perspective. *Chem Soc Rev* **2009,** 38, 2565-2575.

3. Whittingham, M. S., Lithium batteries and cathode materials. *Chem Rev* **2004,** 104, 4271-4301.

4. Etacheri, V.; Marom, R.; Elazari, R.; Salitra, G.; Aurbach, D., Challenges in the development of advanced Li-ion batteries: a review. *Energ Environ Sci* **2011,** 4, 3243-3262.

5. Xia, Y., Development of Low Cost Cathode Materials for Lithium-ion Batteries. **2008**.

6. Prosini, P. P.; Zane, D.; Pasquali, M., Improved electrochemical performance of a LiFePO4-based composite cathode. *Electrochim Acta* **2001,** 46, 3517-3523.

7. Yang, S. F.; Song, Y. N.; Ngala, K.; Zavalij, P. Y.; Whittingham, M. S., Performance of LiFePO4 as lithium battery cathode and comparison with manganese and vanadium oxides. *J Power Sources* **2003,** 119, 239-246.

8. Nuli, Y.; Guo, Z. P.; Liu, H. K.; Yang, J., A new class of cathode materials for rechargeable magnesium batteries: Organosulfur compounds based on sulfur-sulfur bonds. *Electrochem Commun* **2007,** 9, 1913-1917.

9. Koshika, K.; Chikushi, N.; Sano, N.; Oyaizu, K.; Nishide, H., A TEMPO-substituted polyacrylamide as a new cathode material: an organic rechargeable device composed of polymer electrodes and aqueous electrolyte. *Green Chem* **2010,** 12, 1573-1575.

10. Choi, W.; Harada, D.; Oyaizu, K.; Nishide, H., Aqueous Electrochemistry of Poly(vinylanthraquinone) for Anode-Active Materials in High-Density and Rechargeable Polymer/Air Batteries. *J Am Chem Soc* **2011,** 133, 19839-19843.

11. Manuel, J.; Kim, J. K.; Matic, A.; Jacobsson, P.; Chauhan, G. S.; Ha, J. K.; Cho, K. K.; Ahn, J. H., Electrochemical properties of lithium polymer batteries with doped polyaniline as cathode material. *Mater Res Bull* **2012,** 47, 2815-2818.

12. Otero, T. F.; Cantero, I., Conducting polymers as positive electrodes in rechargeable lithium-ion batteries. *J Power Sources* **1999,** 81, 838-841.

13. Naoi, K.; Kawase, K.; Mori, M.; Komiyama, M., Electrochemistry of poly(2,2'-dithiodianiline): A new class of high energy conducting polymer interconnected with S-S bonds. *J Electrochem Soc* **1997,** 144, L173-L175.

14. Oyama, N.; Tatsuma, T.; Sato, T.; Sotomura, T., Dimercaptan-Polyaniline Composite Electrodes for Lithium Batteries with High-Energy Density. *Nature* **1995,** 373, 598-600.

15. Oyaizu, K.; Hatemata, A.; Choi, W.; Nishide, H., Redox-active polyimide/carbon nanocomposite electrodes for reversible charge storage at negative potentials: expanding the functional

horizon of polyimides. *J Mater Chem* **2010,** 20, 5404-5410.

16. Killian, J. G.; Coffey, B. M.; Gao, F.; Poehler, T. O.; Searson, P. C., Polypyrrole composite electrodes in an all-polymer battery system. *J Electrochem Soc* **1996,** 143, 936-942.

17. Coffey, B.; Madsen, P. V.; Poehler, T. O.; Searson, P. C., High Charge-Density Conducting Polymer Graphite Fiber-Composite Electrodes for Battery Applications. *J Electrochem Soc* **1995,** 142, 321-325.

18. Suga, T.; Konishi, H.; Nishide, H., Photocrosslinked nitroxide polymer cathode-active materials for application in an organic-based paper battery. *Chem Commun* **2007**, 1730-1732.

19. Nakahara, K.; Iriyama, J.; Iwasa, S.; Suguro, M.; Satoh, M.; Cairns, E. J., Cell properties for modified PTMA cathodes of organic radical batteries. *J Power Sources* **2007,** 165, 398-402.

20. Guo, W.; Yin, Y. X.; Xin, S.; Guo, Y. G.; Wan, L. J., Superior radical polymer cathode material with a two-electron process redox reaction promoted by graphene. *Energ Environ Sci* **2012,** 5, 5221-5225.

21. Nakahara, K.; Iwasa, S.; Satoh, M.; Morioka, Y.; Iriyama, J.; Suguro, M.; Hasegawa, E., Rechargeable batteries with organic radical cathodes. *Chem Phys Lett* **2002,** 359, 351-354.

22. Kim, J. K.; Cheruvally, G.; Choi, J. W.; Ahn, J. H.; Lee, S. H.; Choi, D. S.; Song, C. E., Effect of radical polymer cathode thickness on the electrochemical performance of organic radical battery. *Solid State Ionics* **2007,** 178, 1546-1551.

23. Suga, T.; Ohshiro, H.; Sugita, S.; Oyaizu, K.; Nishide, H., Emerging N-Type Redox-Active Radical Polymer for a Totally Organic Polymer-Based Rechargeable Battery. *Adv Mater* **2009,** 21, 1627-1630.

24. Oyaizu, K.; Nishide, H., Radical Polymers for Organic Electronic Devices: A Radical Departure from Conjugated Polymers? *Adv Mater* **2009,** 21, 2339-2344.

25. Lee, S. H.; Kim, J. K.; Cheruvally, G.; Choi, J. W.; Ahn, J. H.; Chauhan, G. S.; Song, C. E., Electrochemical properties of new organic radical materials for lithium secondary batteries. *J Power Sources* **2008,** 184, 503-507.

26. Katstumata, T.; Qu, J. Q.; Shiotsuki, M.; Satoh, M.; Wada, J.; Igarashi, J.; Mizoguchi, K.; Masuda, T., Synthesis, characterization, and charge/discharge properties of polynorbornenes carrying 2,2,6,6-tetramethylpiperidine-1-oxy radicals at high density. *Macromolecules* **2008,** 41, 1175-1183.

27. Han, X. Y.; Chang, C. X.; Yuan, L. J.; Sun, T. L.; Sun, J. T., Aromatic carbonyl derivative polymers as high-performance Li-ion storage materials. *Adv Mater* **2007,** 19, 1616-1621.

28. Armand, M.; Grugeon, S.; Vezin, H.; Laruelle, S.; Ribiere, P.; Poizot, P.; Tarascon, J. M., Conjugated dicarboxylate anodes for Li-ion batteries. *Nat Mater* **2009,** 8, 120-125.

29. Williams, D. L.; Byrne, J. J.; Driscoll, J. S., A High Energy Density Lithium/Dichloroisocyanuric Acid Battery System. *J Electrochem Soc* **1969,** 116, 2-4.

30. Yao, M.; Senoh, H.; Yamazaki, S.; Siroma, Z.; Sakai, T.; Yasuda, K., High-capacity organic positive-electrode material based on a benzoquinone derivative for use in rechargeable lithium batteries. *J Power Sources* **2010,** 195, 8336-8340.

31. Yao, M.; Araki, M.; Senoh, H.; Yamazaki, S.; Sakai, T.; Yasuda, K., Indigo Dye as a Positive-electrode Material for Rechargeable Lithium Batteries. *Chem Lett* **2010,** 39, 950-952.

32. Haringer, D.; Novak, P.; Haas, O.; Piro, B.; Pham, M. C., Poly(5-amino-1,4-naphthoquinone), a novel lithium-inserting electroactive polymer with high specific charge. *J Electrochem Soc* **1999,** 146, 2393-2396.

33. Song, Z. P.; Zhan, H.; Zhou, Y. H., Anthraquinone based polymer as high performance cathode material for rechargeable lithium batteries. *Chem Commun* **2009**, 448-450.

34. Song, Z. P.; Xu, T.; Gordin, M. L.; Jiang, Y. B.; Bae, I. T.; Xiao, Q. F.; Zhan, H.; Liu, J.; Wang, D. H., Polymer-Graphene Nanocomposites as Ultrafast-Charge and -Discharge Cathodes for Rechargeable Lithium Batteries. *Nano Lett* **2012,** 12, 2205-2211.

35. Le Gall, T.; Reiman, K. H.; Grossel, M. C.; Owen, J. R., Poly(2,5-dihydroxy-1,4-benzoquinone-3,6-methylene): a new organic polymer as positive electrode material for rechargeable lithium batteries. *J Power Sources* **2003,** 119, 316-320.

36. Liu, K.; Zheng, J. M.; Zhong, G. M.; Yang, Y., Poly(2,5-dihydroxy-1,4-benzoquinonyl sulfide) (PDBS) as a cathode material for lithium ion batteries. *J Mater Chem* **2011,** 21, 4125-4131.

37. Foos, J. S.; Erker, S. M.; Rembetsy, L. M., Synthesis and Characterization of Semiconductive Poly-1,4-Dimethoxybenzene and Its Derived Polyquinone. *J Electrochem Soc* **1986,** 133, 836-841.

38. Pirnat, K.; Dominko, R.; Cerc-Korosec, R.; Mali, G.; Genorio, B.; Gaberscek, M., Electrochemically stabilised quinone based electrode composites for Li-ion batteries. *J Power Sources* **2012,** 199, 308-314.

39. Yao, M.; Senoh, H.; Sakai, T.; Kiyobayashi, T., 5,7,12,14-Pentacenetetrone as a High-Capacity Organic Positive-Electrode Material for Use in Rechargeable Lithium Batteries. *Int J Electrochem Sc* **2011,** 6, 2905-2911.

40. Nigrey, P. J.; Macinnes, D.; Nairns, D. P.; Macdiarmid, A. G.; Heeger, A. J., Lightweight Rechargeable Storage Batteries Using Polyacetylene, (Ch)X as the Cathode-Active Material. *J Electrochem Soc* **1981,** 128, 1651-1654.

41. Cheng, F. Y.; Tang, W.; Li, C. S.; Chen, J.; Liu, H. K.; Shen, P. W.; Dou, S. X., Conducting poly(aniline) nanotubes and nanofibers: Controlled synthesis and application in lithium/poly(aniline) rechargeable batteries. *Chem-Eur J* **2006,** 12, 3082-3088.

42. MacDiarmid, A. G., "Synthetic metals": a novel role for organic polymers. *Curr Appl Phys* **2001,** 1, 269-279.

43. Shirakawa, H., The discovery of polyacetylene film - The dawning of an era of conducting

polymers. *Synthetic Met* **2001,** 125, 3-10.

44. Heeger, A. J., Semiconducting and metallic polymers: the fourth generation of polymeric materials. *Synthetic Met* **2001,** 125, 23-42.

45. Nishizawa, M.; Mukai, K.; Kuwabata, S.; Martin, C. R.; Yoneyama, H., Template synthesis of polypyrrole-coated spinel LiMn2O4 nanotubules and their properties as cathode active materials for lithium batteries. *J Electrochem Soc* **1997,** 144, 1923-1927.

46. Che, G. L.; Lakshmi, B. B.; Fisher, E. R.; Martin, C. R., Carbon nanotubule membranes for electrochemical energy storage and production. *Nature* **1998,** 393, 346-349.

47. Bueno, P. R.; Leite, E. R., Nanostructured Li ion insertion electrodes. 1. Discussion on fast transport and short path for ion diffusion. *J Phys Chem B* **2003,** 107, 8868-8877.

48. Bueno, P. R.; Leite, E. R.; Giraldi, T. R.; Bulhoes, L. O. S.; Longo, E., Nanostructured Li ion insertion electrodes. 2. Tin dioxide nanocrystalline layers and discussion on "nanoscale effect". *J Phys Chem B* **2003,** 107, 8878-8883.

49. Suga, T.; Pu, Y. J.; Oyaizu, K.; Nishide, H., Electron-transfer kinetics of nitroxide radicals as an electrode-active material. *B Chem Soc Jpn* **2004,** 77, 2203-2204.

50. Barriga, S., 2,2,6,6-Tetramethylpiperidin-1-oxyl (TEMPO). *Synlett* **2001**, 563-563.

51. Nishide, H.; Koshika, K.; Oyaizu, K., Environmentally benign batteries based on organic radical polymers. *Pure Appl Chem* **2009,** 81, 1961-1970.

52. Yonekuta, Y.; Oyaizu, K.; Nishide, H., Structural implication of oxoammonium cations for reversible organic one-electron redox reaction to nitroxide radicals. *Chem Lett* **2007,** 36, 866-867.

53. Choi, W.; Ohtani, S.; Oyaizu, K.; Nishide, H.; Geckeler, K. E., Radical Polymer-Wrapped SWNTs at a Molecular Level: High-Rate Redox Mediation Through a Percolation Network for a Transparent Charge-Storage Material. *Adv Mater* **2011,** 23, 4440-4443.

54. Gomez-Escalonilla, M. J.; Atienzar, P.; Fierro, J. L. G.; Garcia, H.; Langa, F., Heck reaction on single-walled carbon nanotubes. Synthesis and photochemical properties of a wall functionalized SWNT-anthracene derivative. *J Mater Chem* **2008,** 18, 1592-1600.

55. Yuan, W. Z.; Mao, Y.; Zhao, H.; Sun, J. Z.; Xu, H. P.; Jin, J. K.; Zheng, Q.; Tang, B. Z., Electronic interactions and polymer effect in the functionalization and solvation of carbon nanotubes by pyrene- and ferrocene-containing Poly(1-alkyne)s. *Macromolecules* **2008,** 41, 701-707.

56. Kim, S. M.; Jang, J. H.; Kim, K. K.; Park, H. K.; Bae, J. J.; Yu, W. J.; Lee, I. H.; Kim, G.; Loc, D. D.; Kim, U. J.; Lee, E. H.; Shin, H. J.; Choi, J. Y.; Lee, Y. H., Reduction-Controlled Viologen in Bisolvent as an Environmentally Stable n-Type Dopant for Carbon Nanotubes (vol 131, pg 327, 2009). *J Am Chem Soc* **2009,** 131, 5010-5010.

57. Alt, H.; Binder, H.; Sandsted.G; Kohling, A., Investigation into Use of Quinone Compounds for Battery Cathodes. *Electrochim Acta* **1972,** 17, 873-887.

58. Pasquali, M.; Pistoia, G.; Boschi, T.; Tagliatesta, P., Redox Mechanism and Cycling Behavior of Nonylbenzo-Hexaquinone Electrodes in Li Cells. *Solid State Ionics* **1987,** 23, 261-266.

59. Hubert, S.; Pham, M. C.; Dao, L. H.; Piro, B.; Nguyen, Q. A.; Hedayatullah, M., A new functionalized conductive polymer poly(2-methyl-5-amino-1,4-naphthoquinone) (PMANQ) with two distinct redox systems. *Synthetic Met* **2002,** 128, 67-81.

60. Pham, M. C.; Piro, B.; Bazzaoui, E. A.; Hedayatullah, M.; Lacroix, J. C.; Novak, P.; Haas, O., Anodic oxidation of 5-amino-1,4-naphthoquinone (ANQ) and synthesis of a conducting polymer (PANQ). *Synthetic Met* **1998,** 92, 197-205.

61. Chouksey, P.; Chandra, B. P.; Ramrakhiani, M., Electroluminescence of CdS nanoparticles-polyvinyl carbazole composites. *Indian J Eng Mater S* **2009,** 16, 157-160.

62. Klopffer, W., Transfer of Electronic Excitation Energy in Polyvinyl Carbazole. *J Chem Phys* **1969,** 50, 2337-2343.

63. Yao, M.; Senoh, H.; Sakai, T.; Kiyobayashi, T., Redox active poly(N-vinylcarbazole) for use in rechargeable lithium batteries. *J Power Sources* **2012,** 202, 364-368.

64. Ambrose, J. F.; Carpenter, L. L.; Nelson, R. F., Electrochemical and Spectroscopic Properties of Cation Radicals .3. Reaction Pathways of Carbazolium Radical Ions. *J Electrochem Soc* **1975,** 122, 876-894.

65. Compton, R. G.; Davis, F. J.; Grant, S. C., The Anodic-Oxidation of Poly(N-Vinylcarbazole) Films. *J Appl Electrochem* **1986,** 16, 239-249.

66. Hsieh, B. R.; Litt, M. H.; Abbey, K., Poly(N-Acylethylenimines) with Pendant Carbazole Derivatives .3. Electrochemical Studies. *Macromolecules* **1986,** 19, 521-529.

67. Maleki, H.; Deng, G. P.; Anani, A.; Howard, J., Thermal stability studies of Li-ion cells and components. *J Electrochem Soc* **1999,** 146, 3224-3229.

68. Song, H. K.; Palmore, G. T. R., Redox-active polypyrrole: Toward polymer-based batteries. *Adv Mater* **2006,** 18, 1764-1768.

69. Song, H. K.; Lee, E. J.; Oh, S. M., Electrochromism of 2,2'-azinobis(3-ethylbenzothiazoline-6-sulfonate) incorporated into conducting polymer as a dopant. *Chem Mater* **2005,** 17, 2232-2233.

70. Hwang, R. Y.; Kim, S. Y.; Palmore, G. T. R.; Song, H. K., Suppression of the loss of an electroactive dopant from polypyrrole by using a non-aqueous electrolyte of dopant-phobicity. *J Electroanal Chem* **2011,** 657, 181-186.

71. Park, H. S.; Ko, S. J.; Park, J. S.; Kim, J. Y.; Song, H. K., Redox-active charge carriers of conducting polymers as a tuner of conductivity and its potential window. *Sci Rep-Uk* **2013,** 3, 2545-2550.

72. Marks, T.; Trussler, S.; Smith, A. J.; Xiong, D. J.; Dahn, J. R., A Guide to Li-Ion Coin-Cell Electrode Making for Academic Researchers. *J Electrochem Soc* **2011,** 158, A51-A57.

73. Chang Hun Yun, H. S. L., Carbon nanotubes material. *Polymer Science and Technology* **2007,** 18, 4-7.

74. Wang, K.; Zhao, P.; Zhou, X. M.; Wu, H. P.; Wei, Z. X., Flexible supercapacitors based on cloth-supported electrodes of conducting polymer nanowire array/SWCNT composites. *J Mater Chem* **2011,** 21, 16373-16378.

75. Kim, J. K., Micro-fibrous organic radical electrode to improve the electrochemical properties of organic rechargeable batteries. *J Power Sources* **2013,** 242, 683-686.

76. wellcos coin-type half cell. http://www.wlcos.com/.

77. Hill, J. T. J. E. a. H. W. J., *US Pat.* **1963,** 3.

78. Zhang, A. F.; Shu, L. J.; Bo, Z. S.; Schluter, A. D., Dendronized polymers: Recent progress in synthesis. *Macromol Chem Physic* **2003,** 204, 328-339.

79. Chen, Y. M.; Xiong, X. Q., Tailoring dendronized polymers. *Chem Commun* **2010,** 46, 5049-5060.

80. Schluter, A. D.; Rabe, J. P., Dendronized polymers: Synthesis, characterization, assembly at interfaces, and manipulation. *Angew Chem Int Edit* **2000,** 39, 864-883.

81. Li, W.; Wu, D. L.; Schluter, A. D.; Zhang, A. F., Synthesis of an Oligo(ethylene glycol)-Based Third-Generation Thermoresponsive Dendronized Polymer. *J Polym Sci Pol Chem* **2009,** 47, 6630-6640.

82. Kim, J.; Yun, M. H.; Lee, J.; Kim, J. Y.; Wudl, F.; Yang, C., A synthetic approach to a fullerene-rich dendron and its linear polymer via ring-opening metathesis polymerization. *Chem Commun* **2011,** 47, 3078-3080.

83. Marsico, F.; Wagner, M.; Landfester, K.; Wurm, F. R., Unsaturated Polyphosphoesters via Acyclic Diene Metathesis Polymerization. *Macromolecules* **2012,** 45, 8511-8518.

84. Bielawski, C. W.; Grubbs, R. H., Highly efficient ring-opening metathesis polymerization (ROMP) using new ruthenium catalysts containing N-heterocyclic carbene ligands. *Angew Chem Int Edit* **2000,** 39, 2903-2906.

85. Kim, K. O.; Choi, T. L., Synthesis of Rod-Like Dendronized Polymers Containing G4 and G5 Ester Dendrons via Macromonomer Approach by Living ROMP. *Acs Macro Lett.* **2012,** 1, 445-448.

86. Song, Z. P.; Zhan, H.; Zhou, Y. H., Anthraquinone based polymer as high performance cathode material for rechargeable lithium batteries. *Chem. Commun.* **2009**, 448-450.

87. Song, Z. P.; Xu, T.; Gordin, M. L.; Jiang, Y. B.; Bae, I. T.; Xiao, Q. F.; Zhan, H.; Liu, J.; Wang, D. H., Polymer-Graphene Nanocomposites as Ultrafast-Charge and -Discharge Cathodes for Rechargeable Lithium Batteries. *Nano Lett.* **2012,** 12, 2205-2211.

88. Choi, W.; Harada, D.; Oyaizu, K.; Nishide, H., Aqueous Electrochemistry of Poly(vinylanthraquinone) for Anode-Active Materials in High-Density and Rechargeable Polymer/Air

Batteries. *J. Am. Chem. Soc.* **2011,** 133, 19839-19843.